

# **Stability and Dynamic Processes in the Formation of High Plains Hailstorms**

By  
David S. Renne

Department of Atmospheric Science  
Colorado State University  
Fort Collins, Colorado

Prepared with support from the National Science Foundation  
Grant No. GA-1561  
Principal Investigator, Peter C. Sinclair  
February, 1969



**Department of  
Atmospheric Science**

Paper No. 136

STABILITY AND DYNAMIC PROCESSES IN THE FORMATION  
OF HIGH PLAINS HAILSTORMS

by  
David S. Renne

This report was prepared with support from  
the National Science Foundation  
Grant No. GA-1561  
Principal Investigator, Peter C. Sinclair

Department of Atmospheric Science  
Colorado State University  
Fort Collins, Colorado

February, 1969

Atmospheric Science Paper No. 136

## ABSTRACT

The structure of a hail-producing and no hail-producing atmosphere is studied by examining rawinsondes launched at New Raymer, Colorado, in the summer of 1967. It is found through examination of mean soundings and the convective condensation level and level of free convection that an ample low-level moisture supply is important for hailstorms to form. The lifted index is a useful parameter for determining the degree of convective instability. A Total Energy Index is derived from energy profiles of  $C_p T + gZ + Lw$ , and this index is also shown to be a good indicator of the degree of potential instability.

An increase in baroclinicity on a large scale occurs when summertime hailstorms form. Furthermore, it is shown that the occurrence of hail is related to a surface convergence mechanism. The resulting circulation can advect Gulf moisture into the region from the east and south, resulting in an increase in instability. The effects of atmospheric destabilization through horizontal temperature advection are examined, but the results are doubtful due to sparseness of data and instrument and analysis errors.

The results of the 1967 data are applied to the forecasting of a few cases of hail and no hail occurrences in 1968.

David S. Renne  
Department of Atmospheric Science  
Colorado State University  
February, 1969

## ACKNOWLEDGEMENTS

The author wishes to express his appreciation to Professor Peter C. Sinclair for his guidance and counsel during this research. Thanks are also due to Professors William M. Gray and Herman Koloseus for serving on the graduate committee. The help in compiling and reducing the data by Miss Marilyn Warren and the typing of the manuscript by Miss Marjorie Allan is deeply appreciated. The helpful discussions with Mr. Charles Chappell and Mr. Thomas Wills are particularly valued.

A sincere thanks is extended to my wife, Linda, whose constant assistance and encouragement during this period of research has been extremely helpful in the completion of this paper.

This project was completed under the sponsorship of the National Science Foundation Grant GA-1561.

This material is based upon a thesis submitted as partial fulfillment of the requirements for the Master of Science Degree at Colorado State University.

TABLE OF CONTENTS

	Page
TITLE PAGE . . . . .	i
ABSTRACT . . . . .	ii
ACKNOWLEDGEMENTS . . . . .	iii
LIST OF TABLES . . . . .	v
LIST OF FIGURES . . . . .	vi
CHAPTER I: INTRODUCTION . . . . .	1
Statement of Problem . . . . .	1
Data Sources for the Colorado State University Hail Project . . . . .	2
Procedure of Investigation . . . . .	2
CHAPTER II: USE OF THE UPPER AIR SOUNDING IN HAILSTORM STUDIES . . . . .	3
Mean Soundings for Hail and no Hail Days . . . . .	3
Specific Features of the Vertical Stratification . . . . .	6
Moisture . . . . .	6
The Convective Condensation Level (CCL) and the Level of Free Convection (LFC) . . . . .	8
The Wet Bulb Freezing Level . . . . .	11
The Lifted Index . . . . .	11
The Total Energy Index . . . . .	13
CHAPTER III: DYNAMIC INFLUENCES ON THE FORMATION OF HAIL- STORMS . . . . .	23
Upper-air Disturbances . . . . .	23
Surface Features . . . . .	27
CHAPTER IV: THE EFFECT OF ATMOSPHERIC DESTABILIZATION THROUGH HORIZONTAL TEMPERATURE ADVECTION . . . . .	32
CHAPTER V: APPLICATION OF RESULTS TO HAIL FORECASTING . . . . .	37
Summary of Results . . . . .	37
Application of Results to Specific 1968 Cases . . . . .	38
CHAPTER VI: CONCLUSIONS . . . . .	49
LITERATURE CITED . . . . .	51

LIST OF TABLES

TABLE	PAGE
1. Mean lapse rates for the Denver sounding and the six daily classifications for the New Raymer sounding . . . . .	5
2. Per cent of surface moisture at cloud base as computed from measured cloud bases . . . . .	7
3. Contingency table for CCL . . . . .	10
4. Contingency table for surface moisture . . . . .	20
5. Contingency table for 500 mb moisture . . . . .	20
6. Contingency table for Total Energy Index . . . . .	21
7. Summary of data presented in Figures 10a and 10b showing occurrences of troughs, ridges, and short waves in connection with the Total Energy Index and the formation of hail . . . . .	25
8. Number of cases of each classification based on Figures 13a-d . . . . .	31
9. Forecast Table for 22 June, 1968 . . . . .	38
10. Forecast Table for 1 July, 1968 . . . . .	39
11. Forecast Table for 3 July, 1968 . . . . .	39
12. Forecast Table for 17 July, 1968 . . . . .	40
13. Forecast Table for 19 July, 1968 . . . . .	40
14. Forecast Table for 28 July, 1968 . . . . .	41
15. Summary of results of the Forecasting Tables for the six independent 1968 cases . . . . .	41

## LIST OF FIGURES

FIGURE	PAGE
1. Mean afternoon soundings for each classification for New Raymer, and the mean Denver hail sounding . . . . .	4
2. The convective condensation level plotted against the low-level moisture supply . . . . .	9
3. The level of free convection plotted against the low-level moisture supply . . . . .	9
4. Histogram of the number of cases of each hail classification for various ranges of the height of the wet bulb freezing level above the terrain . . . . .	12
5. The lifted index plotted for each daily classification . . . . .	12
6. Mean profiles of total energy, $E_T$ , for each classification . . . . .	15
7. Mean profiles of temperature plotted for each classification . . . . .	17
8. Mean profiles of latent energy plotted for each classification . . . . .	19
9. Total Energy Index plotted for each classification . . . . .	22
10. a-b. Scattergram of 500 mb wind velocity and direction for (a) and (b) no hail days . . . . .	24
11. a. Composite 500 mb map for days with a ridge to the west and on which no hail fell over northeastern Colorado . . . . .	26
11. b. Composite 500 mb map for days with a ridge to the west and on which hail fell over northeastern Colorado . . . . .	26
12. Total Energy Index plotted for each classification for days with and days without a front within or approaching northeastern Colorado . . . . .	28
13. Schematic of surface pressure pattern, typical of summer . . . . .	30
14. Values of horizontal differential temperature advection for 5 August, 1967, 0500 MST, and the surface weather that occurred nine hours later . . . . .	34
15. U. S. Department of Commerce ESSA Weather Bureau surface and 500 mb charts for 22 June, 1968, 0500 MST . . . . .	42

LIST OF FIGURES (continued)

FIGURE	PAGE
16. U. S. Department of Commerce ESSA Weather Bureau surface and 500 mb charts for 1 July, 1968, 0500 MST . . . . .	43
17. U. S. Department of Commerce ESSA Weather Bureau surface and 500 mb charts for 3 July, 1968, 0500 MST . . . . .	44
18. U. S. Department of Commerce ESSA Weather Bureau surface and 500 mb charts for 17 July, 1968, 0500 MST . . . . .	45
19. U. S. Department of Commerce ESSA Weather Bureau surface and 500 mb charts for 19 July, 1968, 0500 MST . . . . .	46
20. U. S. Department of Commerce ESSA Weather Bureau surface and 500 mb charts for 28 July, 1968, 0500 MST . . . . .	47
21. Profiles of equivalent potential temperature $\theta_e$ , °K for the six independent 1968 cases . . . . .	48



## Chapter I

### INTRODUCTION

#### Statement of Problem

Since 1958 the Department of Atmospheric Science at Colorado State University (Ft. Collins) has conducted a research and experimental hail suppression program. From this program considerable data has been collected from the great number of hailstorms that occur within 100 miles of this city. In this paper the structure of the atmosphere that exists when hailstorms form over the high plains will be examined. This information will then be applied to the forecasting of these storms. Emphasis will be placed primarily on the stability of the atmosphere and synoptic scale processes that could change this stability and induce convective activity during the day.

Miller (1967a) has summarized the techniques that should be employed when making severe weather forecasts in the midwestern United States. He places primary importance on vorticity advection as a lifting mechanism necessary to generate hailstorms. Also of major importance is a very unstable sounding with a moist lower layer and preferably, although not necessarily, a dry upper layer. For the severest storms there should be strong vertical wind shear and perhaps an approaching cold front as a lifting mechanism. The wet bulb freezing level should be 8000 feet above the ground for large hail to occur.

Longley and Thompson (1965), in a study of Alberta hailstorms, point out that a combination of these meteorological parameters is necessary for the formation of hail. Beckwith (1956), in a study of hail in the Denver area, stresses the importance of the Rocky Mountains as an elevated heating source to create instability, and the importance of southwest winds at 500 mb for hail to form. Furthermore he notes that nearly half of all hail cases studied occurred within six to thirty-six hours after a frontal passage.

Harrison and Beckwith (1951) point out that upsloping winds from the east, a dew point front creating a region of convergence, and

atmospheric wave effects generated by the Rocky Mountains may be important in hailstorm formation.

Marwitz (1966), in a study of radiosondes launched at New Raymer, Colorado, notes that in general hail is a function of the instability of the atmosphere. However, he observes several exceptions to this rule. He suggests localized air mass modification or other unidentified processes to assist in the formation of hail. It is hypothesized here that horizontal temperature advection may occur to influence the formation of hail by destabilizing the atmosphere. In this paper this parameter will be computed for a select case in an attempt to determine its effect on the stability of the atmosphere and on the formation of hail.

#### Data Sources for the Colorado State University Hail Project

The Hail Project at Colorado State University has over the last few years flown instrumented aircraft around and underneath northeastern Colorado hailstorms for the purpose of measuring atmospheric quantities and conducting hail suppression experiments. The project has also operated M-33 weather radars at Ault and New Raymer, Colorado, maintained rain gauge networks, and employed the services of mobile and cooperative observers. In addition a daily rawinsonde was launched at New Raymer about one to two hours prior to the time of strongest convective activity (about 1200 MST). The information from this rawinsonde is considered to be representative of the stability of a hail-producing atmosphere due to its proximity both in time and location to hailstorm formation.

#### Procedure of Investigation

The New Raymer rawinsonde launchings were investigated for the summer of 1967, and from them were computed various parameters useful to the study of hail. The inter-relationship of these parameters was examined to determine a "structure" of the atmosphere for hail and no hail days. Synoptic influences were also considered. In addition, an attempt is made to examine the effects of horizontal temperature advection on hailstorm formation.

## Chapter II

### USE OF THE UPPER AIR SOUNDING IN HAILSTORM STUDIES

#### Mean Soundings for Hail and no Hail Days

Figures 1a-f give mean soundings based on rawinsondes launched just prior to major convective activity at New Raymer for the summer of 1967. These figures are based on six classifications of weather that occurred during the summer: 1) Large hail (golfball size or greater); 2) Moderate hail (walnut or grape size); 3) Small hail (shot or pea size); 4) Radar echoes, but no reported hail; 5) No reported radar echoes or hail; 6) Upslope precipitation type days. This latter classification is used for days on which a fresh outbreak of mP or cP air has entered the region. The surface northeasterly winds induced by the pressure system often cause lifting of air to condensation due to the upsloping terrain, resulting in showery and foggy conditions in the vicinity of the eastern foothills of the Rocky Mountains.

The classification of a given day is determined from information on cards filled out by cooperative observers describing individual hailstorms. It is also based on crop hail insurance reports, newspaper articles, radar observations at New Raymer, and visual observations by hail project personnel.

The number of afternoon rawinsonde launches available for each classification for the summer of 1967 is as follows: 1) seven rawinsondes, 2) seven rawinsondes, 3) six rawinsondes, 4) nine rawinsondes, 5) seven rawinsondes, and 6) four rawinsondes.

Figures 1a-f also show the mean sounding for 18 Denver hail days (dashed lines) selected at random from the years 1956-1958, as presented by Beckwith (1960). The New Raymer soundings show higher dew points in the very lowest levels with a rapid decrease in the vertical. The New Raymer temperature lapse rates are more stable for all classifications of hail days than those shown by the Denver sounding. The temperature at the lifting condensation level on the Denver sounding is +5°C compared with +12°C, +11°C, and +11°C for large, moderate, and

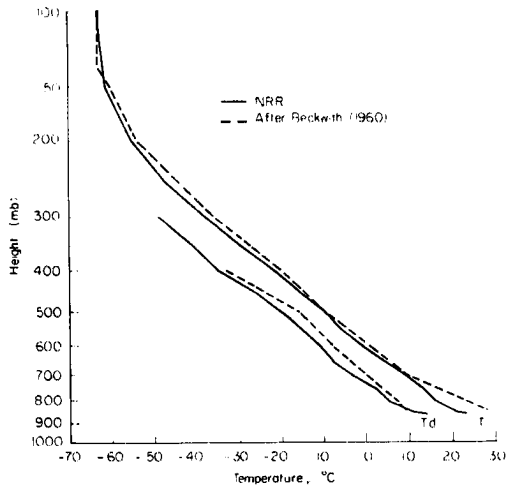


Figure 1a: Large hail (1)

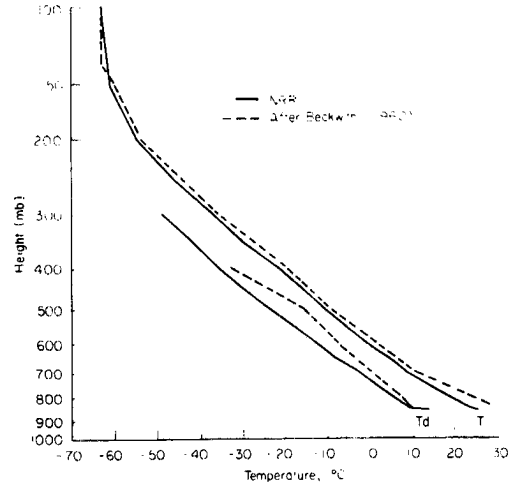


Figure 1b: Moderate hail (2)

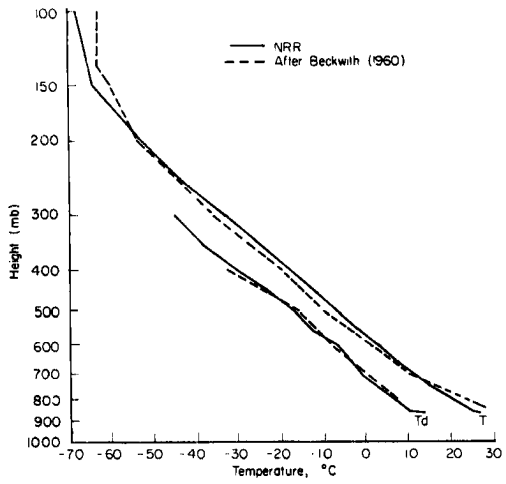


Figure 1c: Small hail (3)

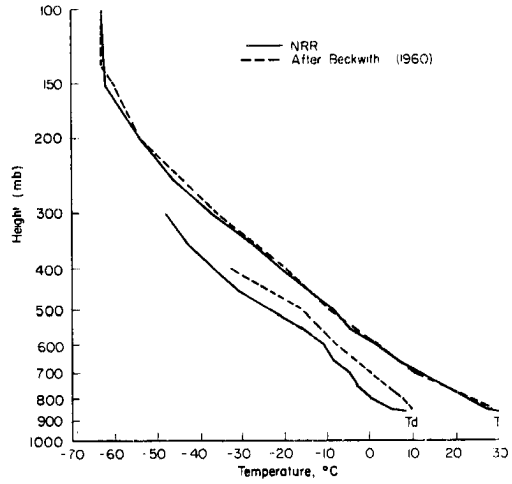


Figure 1d: Radar echoes, no hail (4)

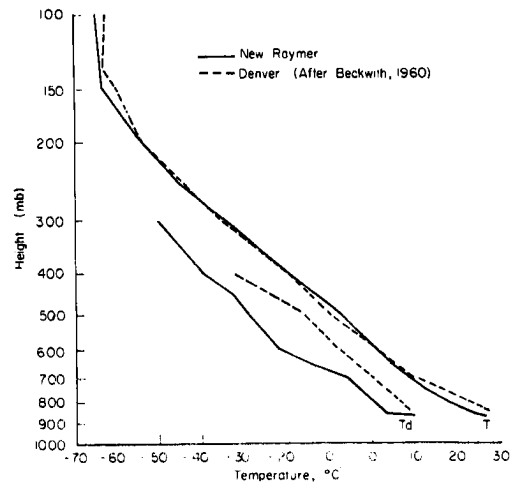


Figure 1e: No echoes or hail (5)

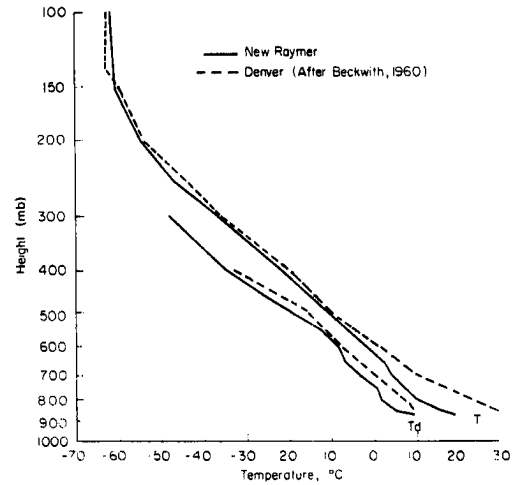


Figure 1f: Upslope precipitation (6)

Figures 1a-f: Mean afternoon soundings for each classification for New Raymer (NRR) and the mean Denver hail sounding from Beckwith (1960). T = temperature,  $T_d$  = dew point.

small hail days on the New Raymer sounding, respectively. These warmer temperatures are due to the high surface dew points observed at New Raymer.

The mean Denver sounding shows an increase in relative humidity up to 500 mb, with a rapid decrease above. This appears to indicate a subsidence inversion at the 500 mb level. This does not show up on the New Raymer sounding for hail days, although it is evident for no hail days (excluding upslope precipitation days). The subsidence region appears to be related to the frequent high pressure ridge over the Rocky Mountain area during the middle and late summer.

The most striking difference between soundings for hail and no hail days at New Raymer is the much greater low-level moisture on hail days. Furthermore, Table 1 shows that, with the exception of the classification of echoes but no reported hail, the temperature lapse rates are steeper for hail than for no hail days. If a parcel is lifted from the surface using the surface parameters shown on these mean soundings, it is seen that on no hail days a much smaller buoyant energy is realized. If entrainment is taken into consideration after saturation, the no hail days have negligible buoyant energy. Thus despite the steep lapse rates for days classified as echoes but no hail, the lack of abundant moisture inhibits strong parcel lifting.

TABLE 1  
Mean lapse rates ( $^{\circ}\text{C}-100 \text{ mb}^{-1}$ ) for the Denver sounding (Beckwith, 1960) and the six daily classifications for the New Raymer soundings.

Level (mb)	Denver Sounding*	New Raymer Sounding					
		(1)	(2)	(3)	(4)	(5)	(6)
850-500	12.6	11.7	12.0	12.7	12.7	12.4	11.0
850-150	11.0	10.6	11.3	10.7	12.0	10.3	9.0

\*Due to the higher terrain, lapse rates are computed from 800-500 mb, and 800-150 mb respectively, for the Denver sounding.

Schleusener (1963) computed mean soundings for heavy, moderate, and no hail days by combining individual soundings of Lander, Scottsbluff, North Platte, Denver, and Goodland for both morning (1200Z) and evening (0000Z) and averaging for each classification. The main difference between the soundings was an increase in low level temperatures and a decrease in low level moisture with a decrease in hail intensity. This is generally in agreement with the soundings presented here.

### Specific Features of the Vertical Stratification

#### Moisture

One of the most crucial factors in analyzing a vertical temperature and moisture sounding is the determination of the low level moisture that could be considered representative of that actually contained in a rising parcel. One procedure as practiced by many forecasters is to take a mean mixing ratio of the lowest 3000 feet (or 100 mb) of the sounding as the representative moisture. However, Fawbush and Miller (1953) point out that the use of the lower 3000 feet of the sounding gives a higher than observed convective condensation level and forecasts hailstone sizes smaller than those observed over the high plains. They claim that better results are obtained in the area from the Continental Divide to the 3000 feet msl level by using the highest mixing ratio observed or forecast at or within 75 mb of the surface.

To determine the representative moisture contained in a lifted parcel, cloud base measurements made available at or near the time and vicinity of the rawinsonde launch from research aircraft operated by the Colorado State University Hail Project were examined. A study was then made to determine a relationship between the surface mixing ratio and the mixing ratio at cloud base.

Actual measured cloud base heights were compared with heights computed from dry adiabatic parcel ascent of surface temperature and moisture conditions measured by the New Raymer hygromograph. Table 2 shows the actual measured cloud base and the calculated cloud base determined from parcel ascent for each case. The surface mixing

ratio needed for the observed cloud base and the actual surface mixing ratio as determined from the hygromograph are presented in columns A and B, respectively. Column C shows the percent difference of these two values. A negative sign means that the cloud base moisture is less than the surface moisture by the given percentage.

TABLE 2  
Per cent of surface moisture at cloud base as  
computed from measured cloud bases.

Actual Observed Base	Computed Cloud Base	A Cloud Base w, gm/kgm	B Surface w, gm/kgm	C % Difference
9.8 Kft	8.7 Kft	10.9	13.5	-19%
10.8 Kft	9.9 Kft	10.3	12.1	-15%
9.2 Kft	8.3 Kft	10.0	11.9	-16%
11.8 Kft	11.7 Kft	12.8	13.1	-2%
10.5 Kft	9.3 Kft	11.0	13.1	-16%
9.4 Kft	9.3 Kft	11.2	11.6	-4%
10.0 Kft	10.3 Kft	10.1	10.4	-3%
11.5 Kft	10.3 Kft	8.4	10.5	-20%
16.0 Kft	15.1 Kft	6.5	7.5	-13%
11.2 Kft	10.6 Kft	10.0	11.0	-9%
15.6 Kft	12.7 Kft	6.2	10.4	-40%
15.9 Kft	14.1 Kft	5.0	6.0	-17%
11.5 Kft	11.1 Kft	9.9	10.1	-2%
12.5 Kft	12.5 Kft	7.6	7.6	0%
14.1 Kft	14.1 Kft	6.2	6.2	0%
10.0 Kft	7.9 Kft	7.3	10.2	-28%
10.3 Kft	8.0 Kft	6.5	9.9	-34%

From Table 2 the average of all observations is -14% with a standard deviation of 4%. Thus, with this limited amount of data, it may be said that 68% of all cloud base computations would require a deficit of surface moisture of  $-14\% \pm 4\%$ , and 95% of all cases would require a deficit of  $-14\% \pm 8\%$ . If an error of  $\pm 500$  feet in measuring

cloud bases is assumed, then an error of  $\pm 8\%$  in computing parcel moisture deficit from the surface dew point results. Thus, if a surface moisture deficit of  $-14\%$  is used, 95% of the time a cloud base within  $\pm 500$  feet of that actually observed may be computed. However, since all bases were measured below cloud base, a systematic error may be introduced such that bases were, if anything, higher than measured. This would tend to underestimate the amount of moisture deficit.

Another possible error is the variation in surface dew points over the region. Variations in surface water content due to lakes, evapotranspiration processes, or uneven mixing of the atmosphere could produce "pockets" of moisture or dry areas that would result in dew points different from surrounding areas. No attempt was made to include these errors here, and the dew points at New Raymer were taken to be representative of the entire region.

This method may be used to determine not only cloud bases, but also the degree of buoyant energy available. This can be done by continuing to lift the parcel on a thermodynamic diagram after it reaches saturation and determine the positive buoyant (or negative non-buoyant) energy by comparing the moist adiabat outlined by this parcel with the environmental temperature.

#### The Convective Condensation Level (CCL) and the Level of Free Convection (LFC)

The convective condensation level is the level at which the mean mixing ratio line intersects the dry bulb curve. If the dry adiabat intersecting the temperature curve at the CCL is followed to the surface, the resulting temperature is the temperature to which the surface air must be warmed before a parcel can rise adiabatically to condensation and then continue to rise moist adiabatically, all under positive energy conditions. Thus, theoretically the lower the CCL the less energy required for strong convection to occur. A plot of CCL vs. the low level moisture (14% less the surface value) for all afternoon soundings launched at New Raymer in 1967 is shown in Figure 2 for the various daily categories.

Figure 2 shows that only small hail occurred for all days with a CCL higher than 640 mb (about 12.7 Kft msl). It also shows that no



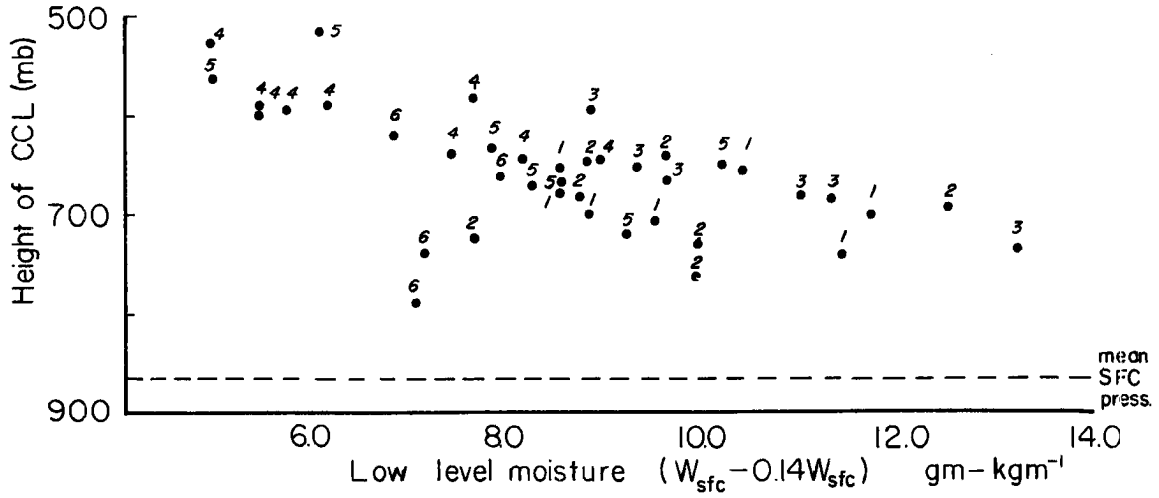


Figure 2: The convective condensation level (CCL) plotted against the low-level moisture supply. The numbers in the scattergram are the daily classification: 1 = large hail, 2 = moderate hail, 3 = small hail, 4 = radar echoes, no hail, 5 = no echoes or hail, 6 = upslope precipitation.

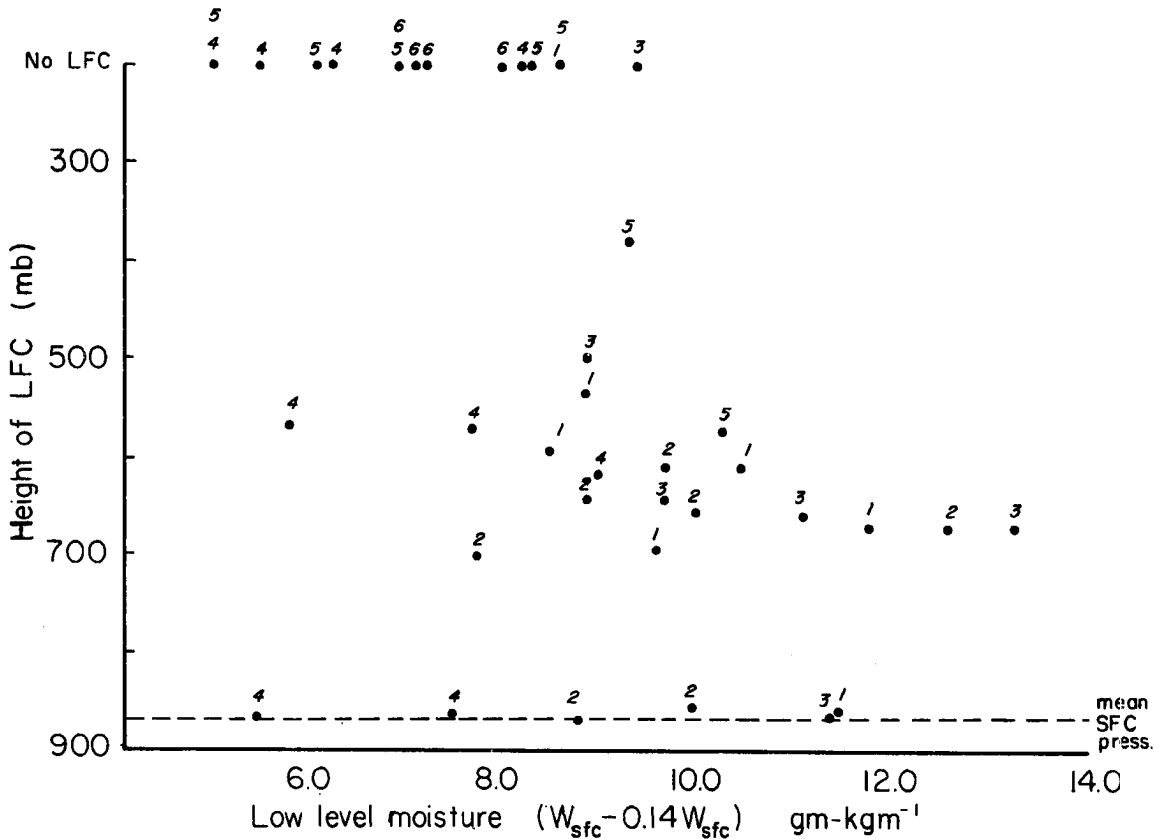


Figure 3: The level of free convection (LFC) plotted against the low level moisture supply. The numbers in the scattergram are the daily classification: 1 = large hail, 2 = moderate hail, 3 = small hail, 4 = radar echoes, no hail, 5 = no echoes or hail, 6 = upslope precipitation.

reported hail fell on days with a mean low level moisture value of less than  $7.6 \text{ gm-kgm}^{-1}$ , although there were scattered cases of reported radar echoes. This is equivalent to a surface dew point of about  $50^{\circ}\text{F}$ . Hail occurred on every day a rawinsonde was launched that gave a mean surface moisture value of greater than  $10.2 \text{ gm-kgm}^{-1}$ . This is equivalent to a surface dew point of  $58^{\circ}\text{F}$ . Although a large number of rawinsondes were launched with a surface dew point between these two extremes, and with all classifications of days, there is a definite trend for high low-level moisture and a low CCL for hail days. The mean surface pressure for the entire summer (862 mb) is included in the diagram.

A contingency table shows further the dependency of a low CCL for the occurrence of hail. These tables are constructed by summing the positive and negative deviations from the average of all data for both hail and no hail days. Table 3 shows that a majority of hail cases occurs with a lower than average CCL, while a majority of no hail cases occurs with a higher than average CCL.

TABLE 3

Contingency table for CCL based on average of 642 mb at New Raymer, Colorado, for Summer of 1967.

---

Hail	17	3
No hail	3	17
	Lower than Average	Higher than Average

---

The level of free convection is the height above which a lifted parcel will remain warmer and more buoyant than the environment. The LFC is very similar to the CCL with the exception that actual surface temperatures are used for the lifted parcel instead of the surface temperatures derived by dry-adiabatic descent from the CCL. The results, shown in Figure 3, are clearly less orderly than the pattern

in Figure 2. This is due most likely to the slight variation in launch times of rawinsondes which, in turn, produce variations in the degree of maximum surface heating that has been reached.

#### The Wet Bulb Freezing Level (WBZ)

The height of the wet bulb freezing level above the ground has been considered important for the size of hail, if any, that will reach the ground. This height is considered to be the freezing level within the cloud. Studies by Miller (1967a) indicate that the optimum height above the ground for the occurrence of large hail with a strong down-rush is 8000 feet, and that if the WBZ is below 5000 feet or above 12,000 feet above the terrain, the chances of hail reaching the ground are very small. Although this is an empirical observation made over the midwestern United States, physically it may be said that a high freezing level within the cloud will hinder the formation of large hailstones, while a low wet bulb zero above the ground indicates a lack of moisture and low-level heating, which may prevent hailstorm formation.

The WBZ was computed for all soundings at New Raymer for 1967. Figure 4 is a histogram of the hail categories for selected ranges of WBZ height above the ground. It shows a preference for large hail to occur with a WBZ between 6000 and 7000 feet above the ground, with large and moderate hail falling with a WBZ between 7000 and 9000 feet above the terrain. These heights are somewhat lower than those shown by Miller (1967a) indicating drier, colder air at the WBZ height for the New Raymer soundings than for most of the soundings investigated by Miller.

The mean Denver sounding for 18 hail days as shown by Beckwith (1960) gives a height of the WBZ of 7500 feet above the terrain, which is more in agreement with the findings of Miller (1967a).

#### The Lifted Index

The lifted index, as defined by Galway (1956) is obtained from a thermodynamic diagram by lifting a parcel dry adiabatically from the modified lower 3000 foot layer next to the ground to saturation. The parcel is then lifted moist adiabatically from saturation to 500 mb. The difference between the environmental dry bulb temperature and

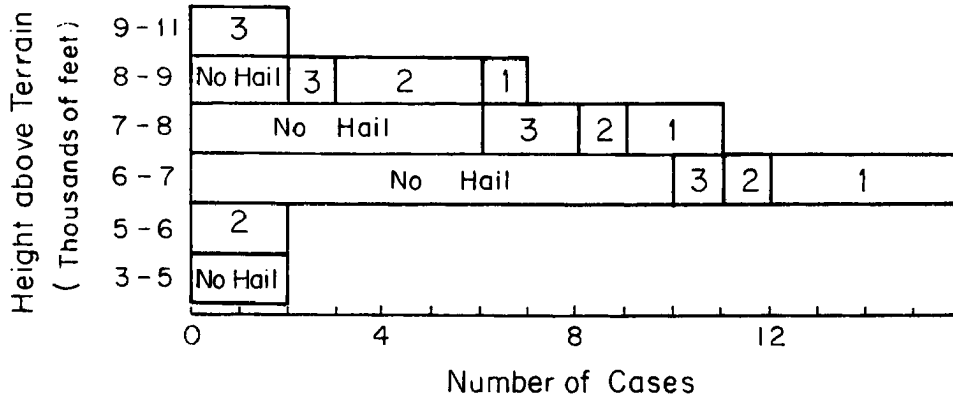


Figure 4: Histogram of the number of cases of each hail classification (numbers within bars) for various ranges of the height of the wet bulb freezing level above the terrain. 1 = large hail, 2 = moderate hail, 3 = small hail.

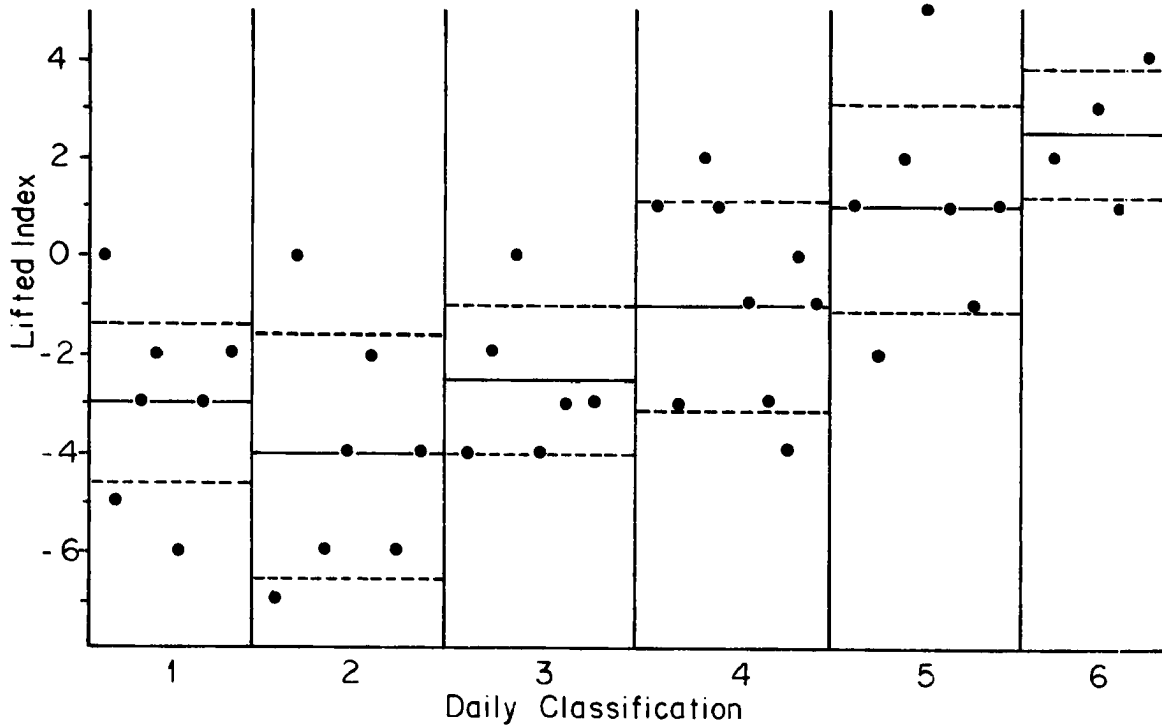


Figure 5: The lifted index plotted for each daily classification. Solid lines are means, dashed lines are the first standard deviations. 1 = large hail, 2 = moderate hail, 3 = small hail, 4 = radar echoes, no hail, 5 = no echoes or hail, 6 = upslope precipitation.

the parcel temperature at 500 mb is called the lifted index. Since the more negative numbers imply more positive buoyant energy at that level, the lifted index is an indicator of the instability of the atmosphere. The lifted index, using the surface moisture less 14%, was computed for all afternoon soundings at New Raymer in 1967 and is presented in Figure 5, along with the mean for each classification (solid lines) and standard deviations (dashed lines).

From Figure 5 it is seen that the large hail days have, in general, the most positive buoyant energy at the 500 mb level. These data suggest that no hail will fall on days with a lifted index less than -2. Miller (1967a), using the lifted index defined by Galway (1956), shows that weak thunderstorm activity may be expected with a lifted index of -2, moderate activity with a lifted index of from -3 to -5, and strong activity with a lifted index of -6.

#### The Total Energy Index

From the equations of motion and the First Law of Thermodynamics the total energy of the atmosphere may be written as (cf. Haltiner and Martin, 1957):

$$\frac{d}{dt} \left( \frac{c^2}{2} + gz + C_p T \right) = \frac{dQ}{dt} + \alpha \frac{\partial P}{\partial t} + \vec{V} \cdot \vec{F} \quad (1)$$

where  $d/dt$  is the derivative with respect to time,  $c$  the wind velocity,  $g$  the gravitational acceleration,  $z$  the height above sea level,  $C_p$  the specific heat of dry air at constant pressure,  $T$  the air temperature,  $dQ$  an increment of heat, and  $\vec{V} \cdot \vec{F}$  the frictional dissipation. For steady, frictionless flow (1) may be written:

$$\frac{d}{dt} \left( \frac{c^2}{2} + gz + C_p T \right) = \frac{dQ}{dt} \quad (2)$$

If the only heat that can be added or removed from the system is the latent heat of condensation,  $dQ = -Ldw$ , where  $w$  is the mixing ratio of the air, and (2) may be written upon integration:

$$\frac{c^2}{2} + gz + C_p T + Lw = \text{const} = E_T \quad (3)$$

where the first term on the left of (3) is the kinetic energy, the second term the geopotential, the third term the enthalpy, and the fourth term the latent energy, all per unit mass.

It is noted that:

$$gz \doteq 980 \text{ cm-sec}^{-2} \times 10^6 \text{ cm} \doteq 100 \text{ joules-gm}^{-1}$$

$$C_p T \doteq 1.004 \text{ joules-gm}^{-1} (\text{°K})^{-1} \times 2.5 \times 10^2 \text{°K} \doteq 250 \text{ joules-gm}^{-1}$$

$$Lw \doteq 2.5 \times 10^3 \text{ joules-gm}^{-1} \times 10^{-2} \doteq 25 \text{ joules-gm}^{-1}$$

$$\frac{c^2}{2} \doteq \frac{(2 \times 10^3 \text{ cm-sec}^{-1})^2}{2} \doteq 0.2 \text{ joules-gm}^{-1}$$

Thus the ratio:

$$\frac{\text{kinetic energy}}{E_T} \doteq \frac{1}{2000}$$

and (3) may be written:

$$C_p T + gz + Lw = E_T \quad (4)$$

Dividing through by  $C_p$  (4) becomes an isobaric equivalent potential temperature,  $\theta_e$ . Using the values  $C_p = 0.24 \text{ cal-gm}^{-1}(\text{°K})^{-1}$ ,  $L = 600 \text{ cal-gm}^{-1}$  (corresponding to a temperature of  $-5^\circ\text{C}$ ), and  $g = 980 \text{ cm-sec}^{-2}$ :

$$\theta_e (\text{°K}) = T (\text{°K}) + 2.5w + 9.8Z \quad (5)$$

where  $w$  is in  $\text{gm-kgm}^{-1}$  and  $Z$  is in km. By substituting numerical values for  $T$ ,  $w$  and  $Z$  in (5) for various levels on a vertical sounding the result is a profile of  $\theta_e$ . Since  $C_p = 1.004 \text{ joules-gm}^{-1}(\text{°K})^{-1}$  the equivalent potential temperature defined in (5) can essentially be expressed as total energy,  $E_T$ .

The isobaric equivalent potential temperature is defined as the temperature attained by a parcel, the moisture of which has been condensed out through an isobaric process, with the release of latent heat used to heat the parcel, and adiabatic descent of the parcel to a reference level of sea level. As demonstrated in Beers (1945) there is a small difference between this and the adiabatic equivalent potential temperature, which is defined as the temperature attained by a parcel after it has been lifted pseudo-adiabatically until all its moisture is condensed out, and then descended dry adiabatically to 1000 mb. Due to the ease of computation of (5), it shall be used here.

Mean profiles for all classifications were computed for the entire summer of 1967, using the New Raymer afternoon soundings. These profiles are shown in Figure 6. Some differences in the structure of the

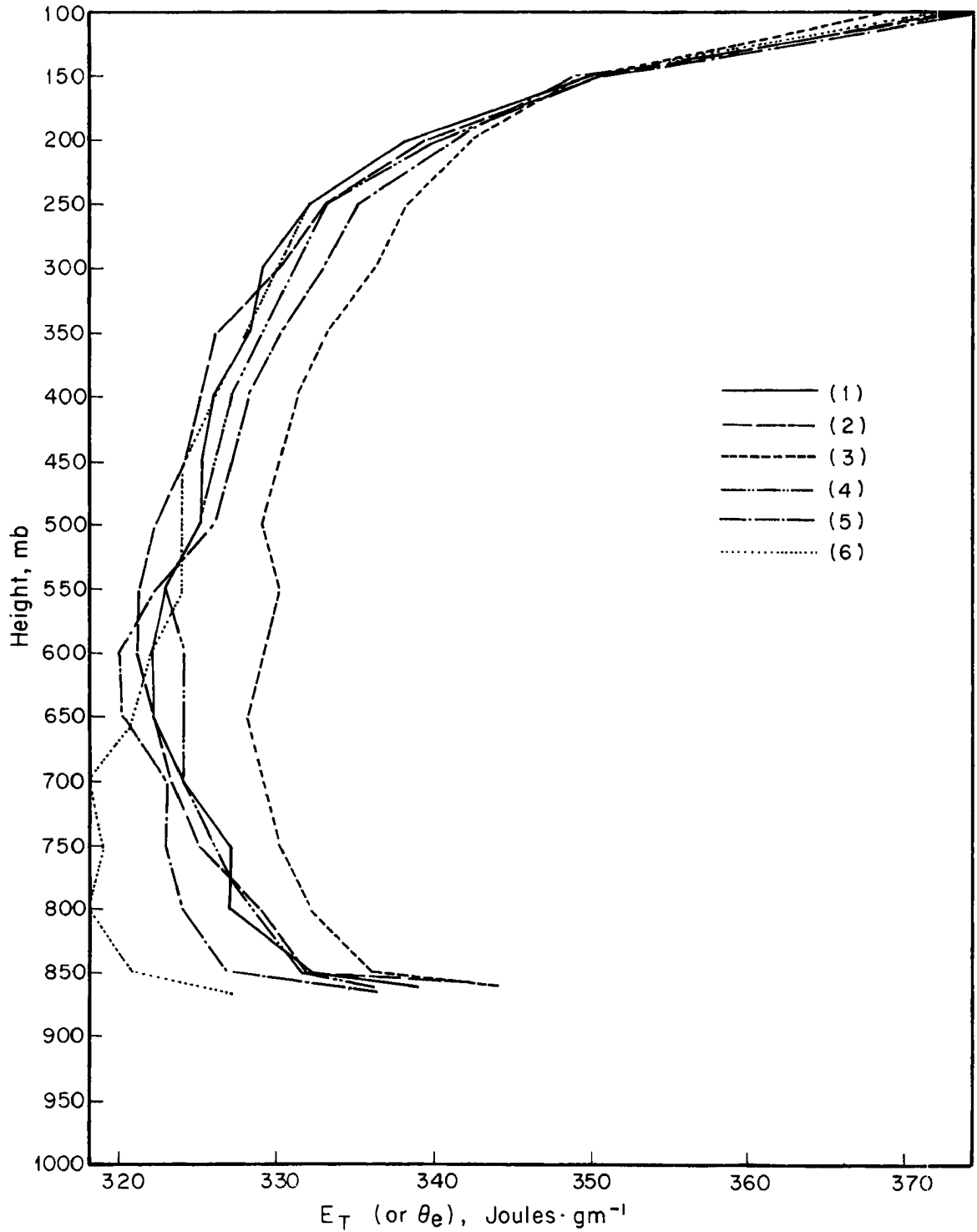


Figure 6: Mean profiles of total energy,  $E_T$  (or equivalent potential temperature,  $\theta_e$ ) for each classification: (1) Large Hail, (2) Moderate Hail, (3) Small Hail, (4) Radar echoes, no hail, (5) No echoes, or hail, (6) Upslope precipitation.

atmosphere between hail and no hail days can be seen from the mean profiles. On hail days, if an undiluted parcel ascends from the surface it rises through constantly decreasing environmental energy up to about 600 mb, when the total environmental energy then increases. No hail days, on the other hand, show a small depression of  $\theta_e$ , and thus a smaller area of positive energy as outlined by an undiluted parcel lifted from the surface.

This decrease of  $\theta_e$  with height is typical of a potentially unstable sounding, as demonstrated by Normand (1938). If a layer in this level is lifted, its lapse rate steepens. Thus for a greater rate of decrease of  $\theta_e$  with height, less lifting is required for the initiation of convective activity.

The minimum equivalent potential temperature, occurring in the mid-troposphere, represents the lowest temperature that can be reached at the earth's surface from the evaporatively cooled saturated downdraft (Normand, 1946). Thus, the difference between the surface maximum  $\theta_e$  and the mid-tropospheric minimum  $\theta_e$  represents the maximum possible energy that can be realized on a potentially unstable sounding.

These curves can be broken up into their individual components to determine which parameter contributes most to the differences between the curves. The difference between values of geopotential is insignificant, and is not presented here.

Figure 7 shows the temperature plotted for the daily classifications. There is very little difference between the curves and consequently only a slight contribution to the difference between the total energy profiles. However, upon close examination of the curves, the lapse rate for no hail days is slightly more stable than for heavy hail days up to just below the tropopause with the exception of the days with echoes but no hail. The days with the warmest low level temperatures produced only small hail or no hail at all. The days with upslope precipitation showed very stable soundings with respect to hail days. The most unstable lapse rate is on days with echoes, but no reported hail. This absence of hail for an unstable lapse rate may be due to the lack of low level moisture, or to the



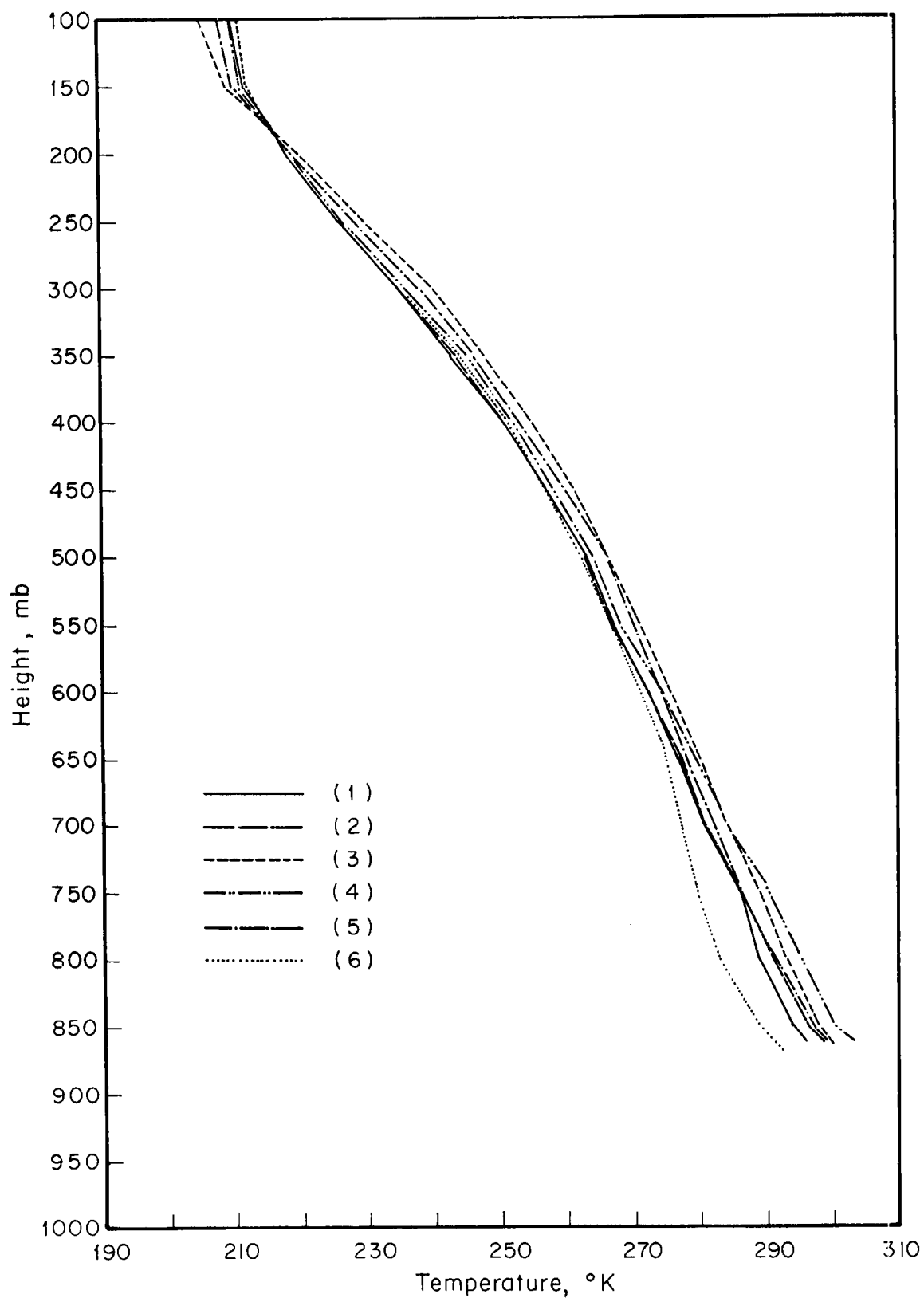


Figure 7: Mean profile of temperature ( $^{\circ}\text{K}$ ) plotted for each classification: (1) Large hail, (2) Moderate hail, (3) Small hail, (4) Radar echoes, no hail, (5) No echoes or hail, (6) Upslope precipitation.

lack of dynamic lifting support, as will be shown later. The variation in these vertical lapse rates can also be seen in Table 1, page 5.

An examination of the curves displaying the contribution to total energy from the available moisture does reveal a striking difference between the classifications, as can be seen in Figure 8. Below 650 mb, which is slightly above the usual convective cloud base, the available moisture is much greater for hail than for no hail days. It is this parameter that contributes to the major difference between the total energy profiles. A greater low-level moisture supply implies a greater release of latent heat when a parcel is lifted to saturation, and consequently greater instability. Furthermore, since this moisture is greater all the way to cloud base and slightly above, a rising parcel will entrain more moist air on hail days than on no hail days and will retain its instability. The air above 400 mb contains approximately the same amount of moisture for both hail and no hail days, with hail days having a slightly greater amount. Thus, for a hail day this represents a rapid decrease in moisture above 400 mb. If large scale lifting occurs, the lapse rate throughout the entire atmosphere will steepen, a case of potential instability. On a thermodynamic diagram these conditions exist when the equivalent potential temperature  $\theta_e$  decreases with height, as mentioned above.

The dependency of high surface moisture on hailstorm formation can be seen further on a contingency table. Table 4 is a contingency table based on a mean surface moisture of  $10.0 \text{ gm-kgm}^{-1}$  (equivalent to a surface dew point of  $11.4^\circ\text{C}$  or  $53^\circ\text{F}$ ). The table shows very strong dependency on above normal low-level moisture and the occurrence of hail.

Table 5 is a contingency table based on the mean moisture at 500 mb of  $1.33 \text{ gm-kgm}^{-1}$  (equivalent to a dew point of  $-22^\circ\text{C}$  or  $-7^\circ\text{F}$ ). This table shows that there is little dependence on the occurrence of hail with abnormalities of 500 mb moisture. For no hail to occur, the moisture should be below average.

Beckwith (1960), in a study of 225 hailstorms over a ten year span in the Denver area, noted that Denver surface dew points higher than  $55^\circ\text{F}$  were rarely observed prior to the occurrence of hailstorms

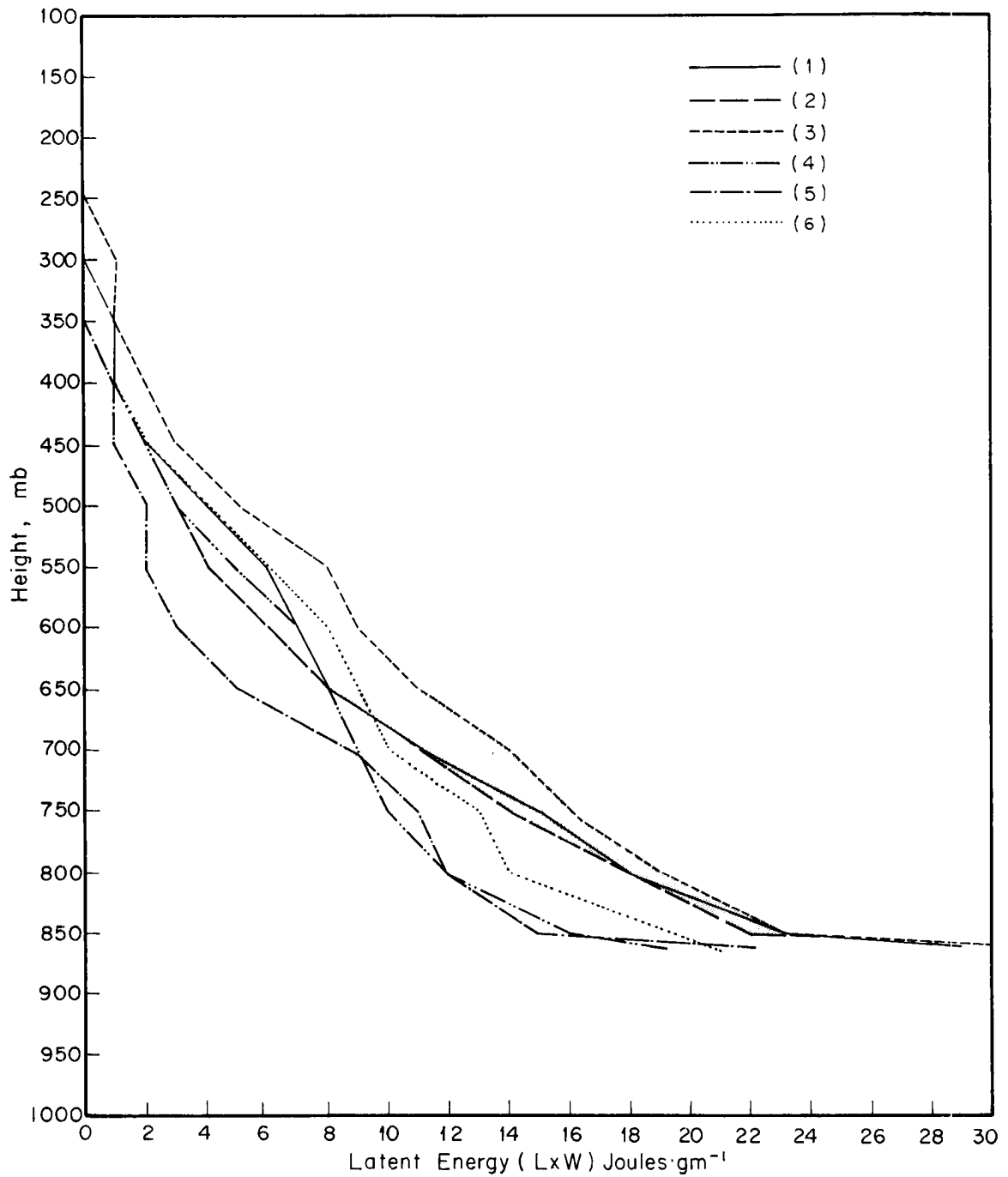


Figure 8: Mean profiles of latent energy ( $Lxw$ ) plotted for each classification: (1) Large hail, (2) Moderate hail, (3) Small hail, (4) Radar echoes, no hail, (5) No echoes or hail, (6) Upslope precipitation. Shaded area encloses the low level moisture for the hail days.

TABLE 4

Contingency table for surface moisture based on average of  $10.0 \text{ gm-kgm}^{-1}$  at New Raymer, Colorado, for summer of 1967.

---

Hail	19	1
No Hail	3	17
	Above Average	Below Average

---

TABLE 5

Contingency table for 500 mb moisture based on average of  $1.33 \text{ gm-kgm}^{-1}$  at New Raymer, Colorado for summer of 1967.

---

Hail	11	9
No Hail	3	17
	Above Average	Below Average

---

and that the average dew point before precipitation began was  $46^{\circ}\text{F}$ . This is in disagreement with the New Raymer data since hail never occurred with dew points of less than  $50^{\circ}\text{F}$ , and the average dew point prior to the occurrence of hail was  $56^{\circ}\text{F}$ . But Denver probably will have lower dew points than New Raymer due to its westward displacement from the source of Gulf maritime moisture.

Thus the crucial factor that causes an atmosphere to yield large positive buoyant energy for an ascending parcel and consequently strong updrafts through a deep layer is an abundant low-level moisture supply.

Total energy profiles were plotted for each afternoon sounding launched at New Raymer in 1967. Energy values were computed for 50 mb intervals in the vertical. An energy index was computed by multiplying the difference between the maximum and minimum values of  $\theta_e$  in the

lower troposphere by the depth of the layer defined by these values. This, in effect, crudely integrates the total possible energy from an atmosphere with warm moist air rising from the surface and evaporatively cooled air descending from the potentially coldest level. The units resulting from this computation will be in joules. This is different from the index proposed by Darkow (1968), where the difference between the 500 mb and 850 mb energy values is utilized.

The index defined here shall be called the Total Energy Index,  $\Delta\theta_e dP$ , where  $\Delta\theta_e$  is the total energy depression (i.e., the total equivalent potential temperature depression), and  $dP$  is the depth of the layer in millibars defined by the total energy depression. Figure 9 gives a scattergram of the Total Energy Index for each classification. Included on this diagram are the mean values for each classification (solid lines) and standard deviations (dashed lines). Furthermore it can be noted that the mean index for all hail days is 5480 joules, compared with 3620 joules for no hail days. A Student's  $t$  test shows that this is a significant difference even for a 0.01 level of significance.

Table 6 is a contingency table for the Total Energy Index, based on a mean for the entire summer of 4550 joules. It shows that although there is a very slight preference of hail falling on days with above normal Index values, there is a high preference for no hail to fall on days with below normal Index values.

TABLE 6

Contingency table for Total Energy Index based on average of 4550 joules at New Raymer, Colorado, for summer of 1967.

Hail	11	9
No Hail	3	17
	Above Average	Below Average

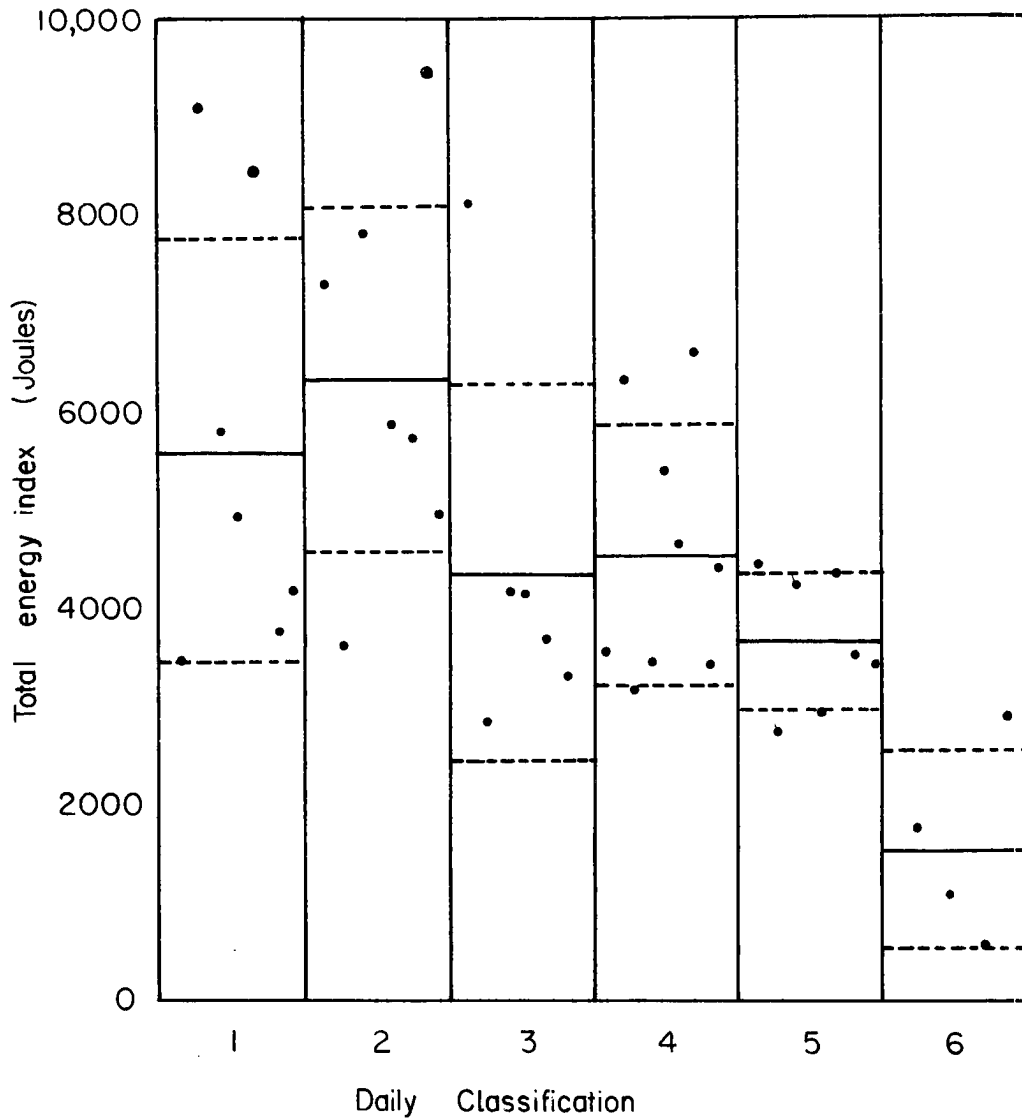


Figure 9: Total energy index plotted for each classification: (1) Large hail, (2) Moderate hail, (3) Small hail, (4) Radar echoes, no hail, (5) No radar echoes or hail, (6) Upslope precipitation. Solid lines are means, dashed lines are the first standard deviation.

Chapter III  
DYNAMIC PROCESSES IN THE FORMATION OF HAILSTORMS

Upper-air Disturbances

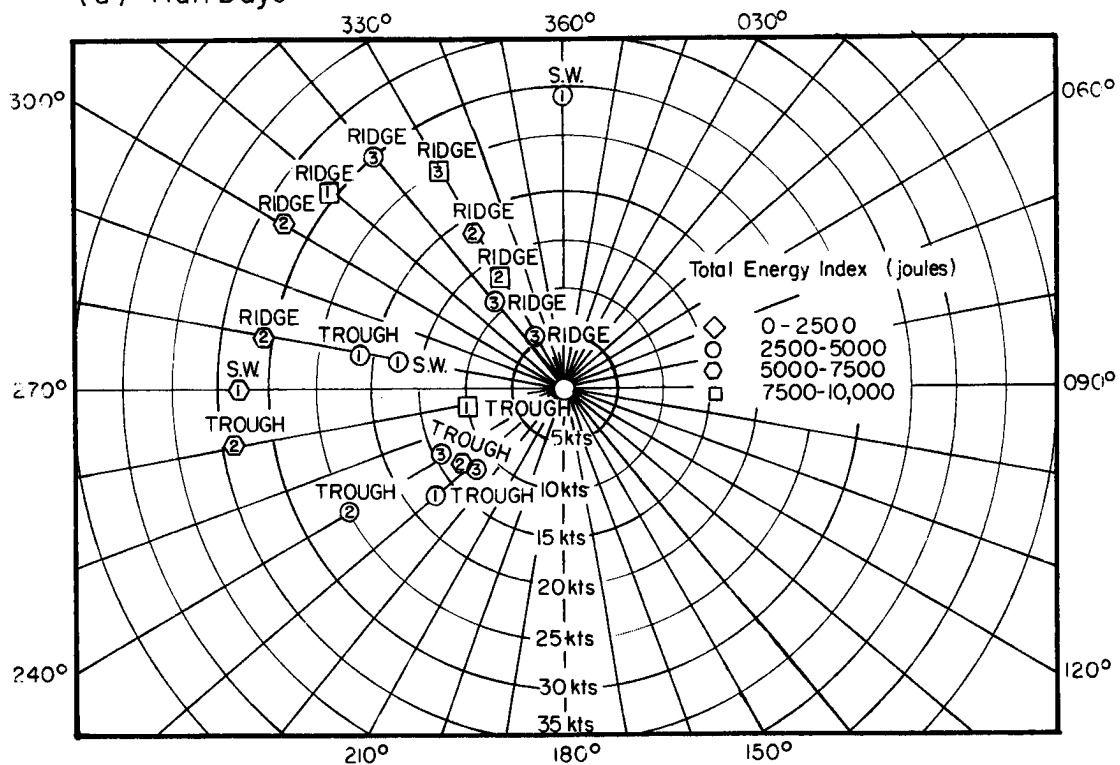
Since the atmosphere is often conditionally unstable, some mechanism must be present that will help lift a parcel through the lower stable layers to saturation until it becomes unstable with respect to the environment. This mechanism may exist in a number of ways, ranging from variations in local terrain to large scale vorticity advection or the passage of a surface front.

Large scale lifting may result from the approach of a trough or short wave from the west. This may be reflected aloft by the direction and strength of the 500 mb winds. Figures 10a and 10b are diagrams of wind velocity and direction for hail and no hail days, respectively, at 500 mb. Included in the figures are geometric symbols representing various ranges of the Total Energy Index,  $\Delta\theta_e dP$ . The numbers enclosed by the symbols are the daily classification. The wind velocity is directly proportional to the distance from the center, and the direction is that from which the wind blows. There is also a note indicating that there was either a long wave trough or ridge to the west, or a short wave perturbation passing over the region.

For the hail cases Figure 10a shows that the degree of atmospheric instability indicated by the Total Energy Index is generally larger when there was a ridge to the west. This implies that there must be slightly greater instability in order for hailstorms to occur with a ridge to the west due possibly to subsidence caused by the ridge. There were very few cases for no hail occurrence with a trough to the west, but when this situation existed, the Total Energy Index was low. Since a ridge is usually situated to the west of the region in late summer, the higher Total Energy values are most likely due to higher surface temperatures and higher surface moisture.

Figure 10b shows that a ridge to the west with only moderate energy values prevailed for no hail days. Occasionally a short wave with relatively higher energy values passed over the region with no

(a) Hail Days



(b) No Hail Days

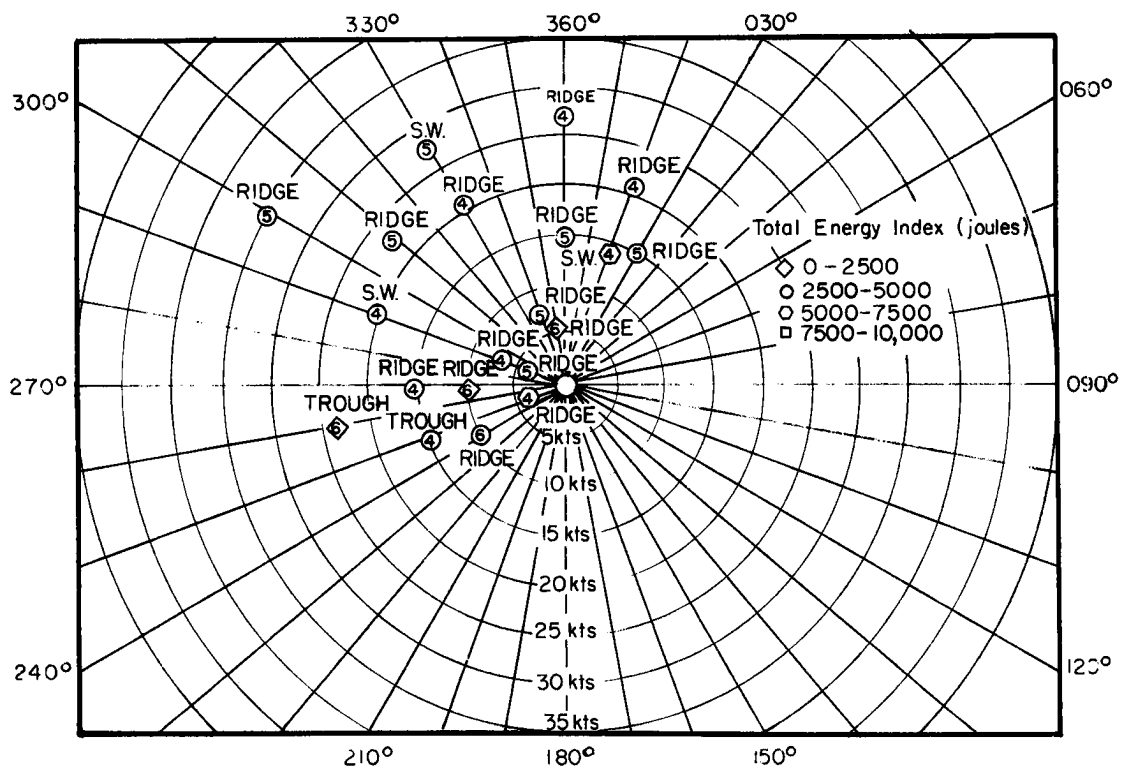


Figure 10a-b: Scattergram of 500 mb wind velocity and direction for (a) hail and (b) no hail days. Included are ranges of the total energy index. Numbers within the symbols are the daily classification.



report of hail. It is possible on days classified as echoes but no reported hail that hail may actually have fallen, yet not reported by any cooperative observer. Table 7 summarizes the data presented in Figures 10a and 10b.

TABLE 7

Summary of data presented in Figures 10a and 10b showing occurrences of troughs, ridges, and short waves in connection with the Total Energy Index and the formation of hail.

	Number of Cases		
	<u>Trough to West</u>	<u>Ridge to West</u>	<u>Short Wave</u>
Hail	○ = 5, ◐ = 1, ◻ = 1	○ = 3, ◐ = 4, ◻ = 3	○ = 2, ◐ = 1
No Hail	◊ = 1, ○ = 1	◊ = 3, ○ = 12, ◐ = 1	○ = 2, ◐ = 1

Composite 500 mb maps for the entire region were constructed for the two cases: no hail occurrences with a ridge to the west of northeastern Colorado and hail occurrences with a ridge to the west. These composite maps are shown in Figures 11a-b.

Figure 11a for no hail cases shows in the mean a small trough to the southeast of the region. There is no temperature advection into northeastern Colorado, although there is considerable crossing of contour lines with isotherms, indicating cold air advection, to the northwest. Over northeastern Colorado there is a geostrophic wind of 20 knots from a direction of 330°.

In Figure 11b for hail days with a ridge to the west there is far greater baroclinicity over northeastern Colorado than Figure 12a shows. A steeper meridional temperature gradient and a stronger geostrophic wind (30 knots from a direction of 305°) with cold air advection over northeastern Colorado is apparent. Thus, even with a ridge established over the region, hail may occur due to an increase in synoptic-scale baroclinicity. This baroclinicity may show up on individual charts as a weak short wave.

Other investigators have also noted an increase in wind speed aloft for hail days. Modahl (1969) shows that wind velocities and

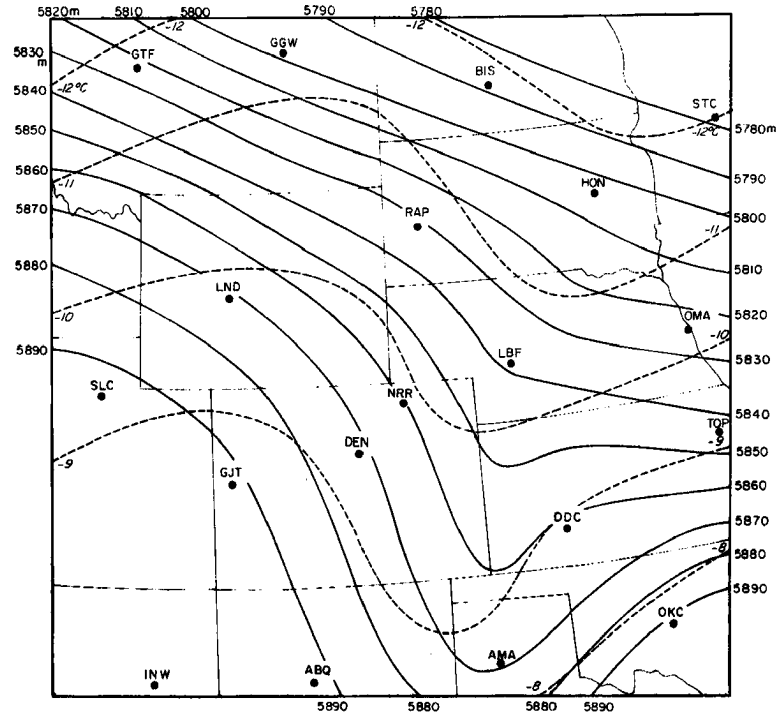


Figure 11a: Composite 500 mb map for days with a ridge to the west and on which no hail fell over northeastern Colorado.

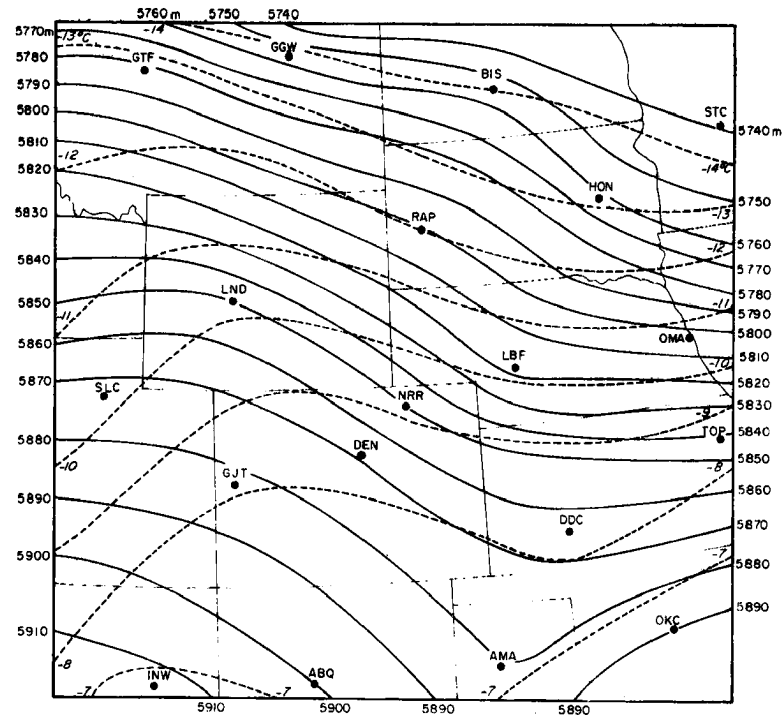


Figure 11b: Composite 500 mb map with a ridge to the west and on which hail was reported over northeastern Colorado.

vertical wind shears generally increase over northeastern Colorado with increasing hail production. Schleusener and Auer (1964) observe stronger winds aloft at all levels over the region for severe hail days, in comparison with moderate and no hail days. Schleusener (1962) observes that hail occurs when a "relative velocity maxima" at 500 mb passes over the region in early spring, and when above average wind velocities exist south of the region in late spring and summer. These observations are based on geostrophic 500 mb winds along the 110° west longitude. Similar observations have been noted in other regions (Dessens, 1960), although some studies show that strong winds aloft do not always exist with hailstorm formation (Ratner, 1961).

In a theoretical study Das (1962) shows that there is a higher probability of hail forming in thundershowers under strong vertical wind shear. Newton and Newton (1959) show that the hydrodynamic pressures caused by the interaction of an environment with strong vertical shear on a cumulonimbus can induce vertical velocities equivalent to those produced by buoyancy forces.

Thus it is seen that the observed strong geostrophic 500 mb winds and the occurrence of hail over northeastern Colorado is in agreement with some theory and most observations.

Composite maps for hail and no hail days with a trough to the west are not presented here due to the wide variation in temperature and contour patterns between individual days. Schleusener and Auer (1964) note that the passage of a trough is often associated with cyclogenesis in southeastern Colorado. The wind pattern caused by this cyclogenesis would bring in Gulf moisture, assisting in convective instability.

#### Surface Features

The presence or passage of a surface front may also be an influence on the formation of hail. The discontinuity can provide enough surface convergence to generate the lifting mechanism necessary on a conditionally unstable day for intense convective activity to occur. These frontal passages are often associated with a short wave or major trough passage aloft.

The data has been stratified for days with and days without the presence of a stationary front or approach of a cold front into the

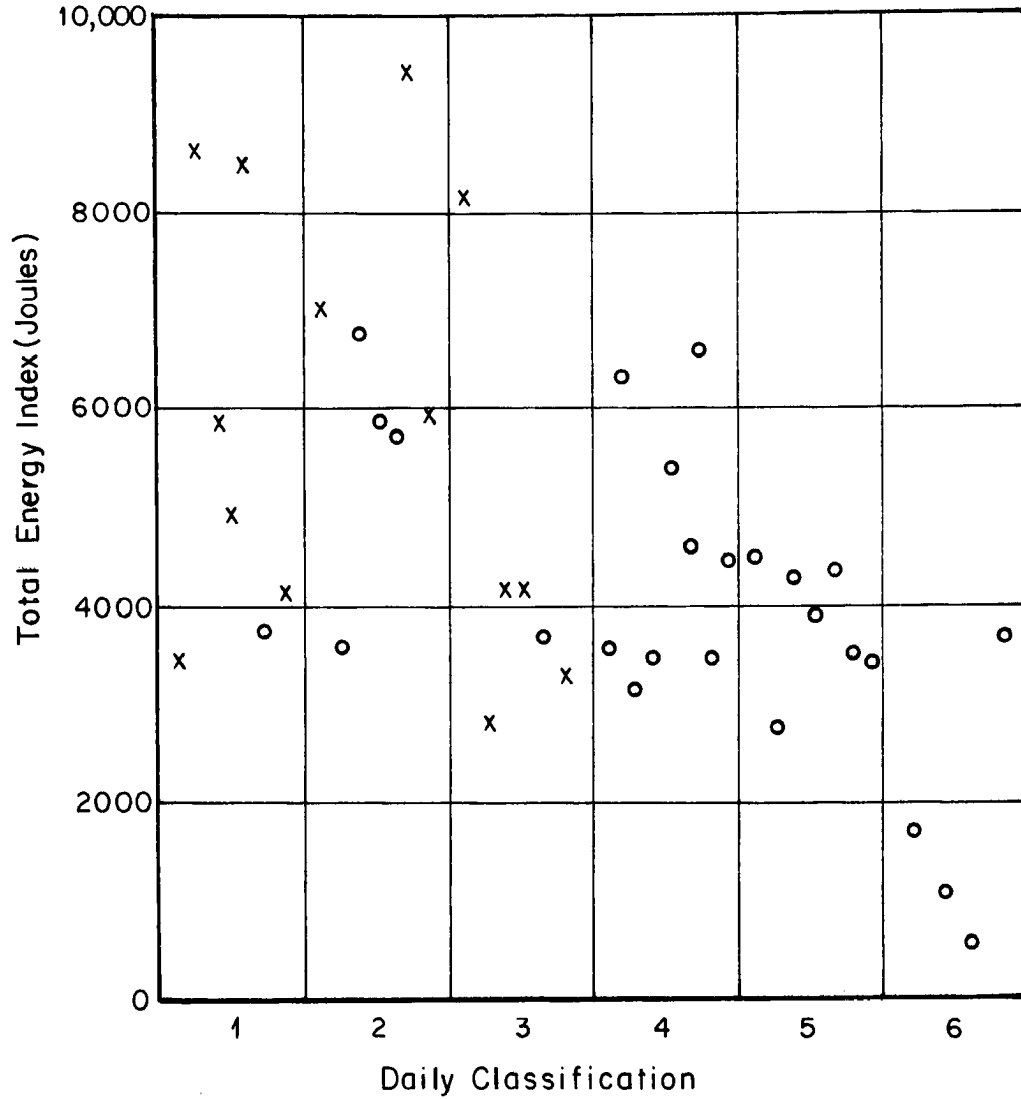


Figure 12: Total Energy Index plotted for each classification for days with a front approaching or within northeastern Colorado (X) and no front approaching or within northeastern Colorado (O).

region. The results of the study, presented in Figure 12, show a very high correlation between the presence of fronts and the occurrence of hail. Only six cases of hail were reported on days with no fronts, and three of these had relatively high Total Energy Index values. Hail did occur on every day with the presence or approach of a front.

Daily surface maps were examined for the entire summer of 1967. Certain patterns of movements of pressure systems became apparent. Schematic surface maps were drawn from these pressure patterns and are shown in Figures 13a-d. The pattern of Figure 13a is typical of days when heavy hail falls on the high plains region. Apparently this is partly due to the lifting created by the general surface vorticity in the region in advance of the front. The cyclonic circulation can further act to advect Gulf moisture into the region, increasing the instability. Since the passage of a surface front is usually associated with an increase in baroclinicity aloft, this increased moisture due to the synoptic features will result in higher Total Energy Values on hail days with a ridge to the west (Figure 10a and 11b).

After the front has passed through, clear, cool weather or upslope precipitation with no hail usually prevails over northeastern Colorado. In the late summer the front may pass on to the northeast after remaining in the area for several days. But often, particularly in the early summer, the cP air mass settles down to the east and southeast of the country, as shown in Figure 13c, with the front drifting to the southern borders of the United States. Then Colorado is under the influence of a "return flow", characterized by weak upsloping winds from the southeast. Depending on how much moisture and heating is brought into the region by this circulation, either thunderstorms with the possibility of some hail or clear weather will prevail. In Figure 13d the cP air mass is merging with the mT air mass, and moisture usually increases over the entire region. After some time a new cold air mass will move into the region, and the cycle starts over again.

Figures 13a and 13d show the dew point front (dashed line) that sometimes occurs to the east of Colorado. This front forms in the

Figure 13a Hail

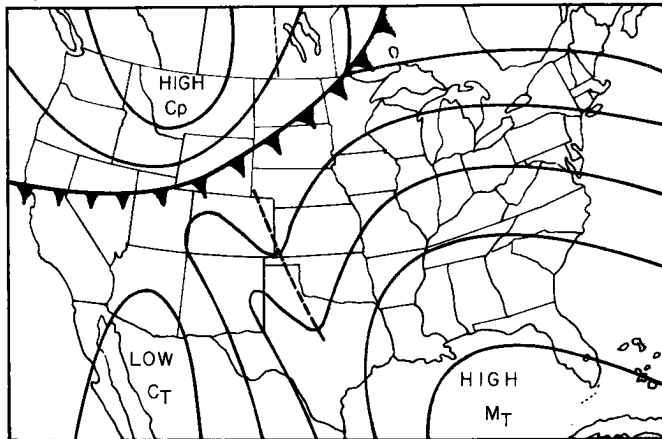


Figure 13c: Hail Thundershowers or Clear ( Depending on low level moisture)

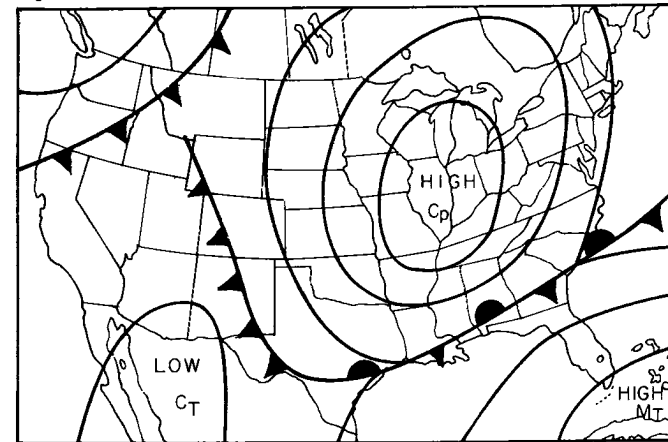


Figure 13 b Clear Weather or Upslope Precipitation

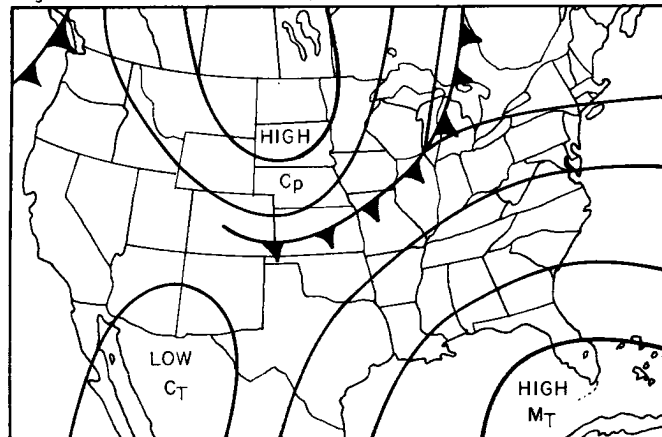


Figure 13 d: Thundershowers with Possible Hail

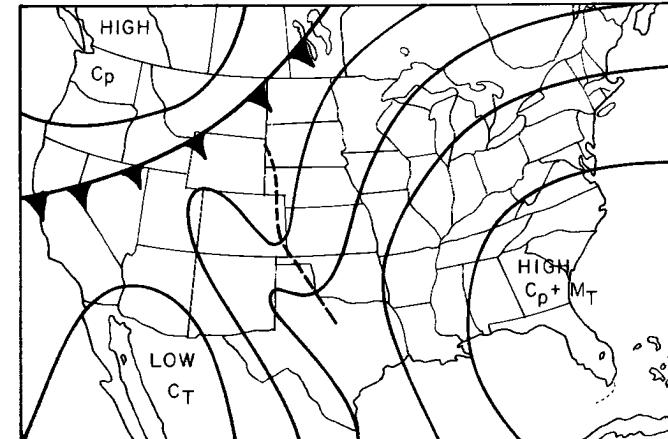


Figure 13a-d: Schematics of surface pressure patterns typical of summer. Above each schematic is the weather that prevails over northeastern Colorado for that particular pattern. The dashed line in Figures 13a and 13d represents the dew point front.

trough that results from the merging of mT air to the east with cT air to the west. This weak zone of convergence may provide enough surface lifting to assist in convection.

Observation shows that pressure patterns similar to those in Figures 13a-d exist for most of the summer with a cycling time that may last anywhere from four to ten days. Table 8 shows the number of cases of hail and no hail that occurred with a surface pattern corresponding to each figure. The results shown here are quite similar to those found in a statistical study of surface weather features for eastern Colorado hailstorms made by Hodges (1959).

TABLE 8

Number of cases of each classification based on Figures 13a-d for 40 cases from the summer of 1967.

	Classification					
	(1)	(2)	(3)	(4)	(5)	(6)
Figure 13a	5	3	3	0	0	0
Figure 13b	0	1	0	2	4	4
Figure 13c	2	2	2	4	3	0
Figure 13d	0	1	1	3	0	0

In summary, it is evident that synoptic-scale processes act not only to provide a lifting mechanism, but to increase the convective instability of the atmosphere. In addition, these large-scale processes result in an increase in vertical wind shear and wind speeds aloft, which act to increase the intensity of large convective systems and induce the formation of large hail.

## Chapter IV

### THE EFFECT OF ATMOSPHERIC DESTABILIZATION THROUGH HORIZONTAL TEMPERATURE ADVECTION

An attempt is made to analyze the effect of vertical destabilization of the atmosphere through the process of horizontal differential temperature advection. Local advective processes may be a means of hailstorm genesis in certain locales even on days with a relatively stable sounding.

On a synoptic scale the temperature tendency equation may be written as:

$$\frac{\partial T}{\partial z} = \frac{1}{C_p} \frac{dQ}{dt} - \vec{V} \cdot \nabla_H T - w(\gamma_d - \gamma) \quad (5)$$

where  $\frac{\partial}{\partial z}$  is the partial derivative in the vertical,  $Q$  is diabatic heating,  $\vec{V}$  the wind velocity vector,  $w$  the vertical velocity,  $\gamma_d$  the dry adiabatic lapse rate, and  $\gamma$  the actual lapse rate.

The first term on the right of (6) represents the diabatic heating of the atmosphere, which may be important near the surface in creating a steep lapse rate and initiating convective activity. The second term on the right is the horizontal advection of temperature, and the third term is the temperature change due to vertical velocities.

House (1958, 1961, 1963) has attempted to show that large scale vertical motions can destabilize an air mass and assist convective activity. However, it is very difficult to compute accurately divergence and kinematic vertical velocities on the meso-scale being considered here using only synoptic scale data. An attempt was made to compute these vertical velocities, but with poor results.

Nevertheless the importance of differential upper and low level advection cannot be discounted, and hence a few sample computations of the term  $-\vec{V} \cdot \nabla_H T$  in equation (6) were made at two levels for a select case, 5 August, 1967. This day is a good example of large hail falling with no apparent large scale synoptic baroclinicity or surface convergence and with a sounding that is only slightly unstable. It can be hypothesized that local destabilization processes



due to differential temperature advection and to low level moisture advection may be the reason for the onset of severe hail activity.

The computations were made on a grid centered over northeastern Colorado, the region of most hail activity. The grid points were spaced approximately 100 statute miles apart, and the network covered the entire state of Colorado, most of southern Wyoming, western Nebraska, and extreme western Kansas. Rawinsonde and pibal information was used, and a network that extended well beyond the borders of the grid was included.

Since several of the rawinsonde launching sites are above the 850 mb level, differential horizontal temperature advection between the 700 mb and 500 mb levels was computed by carefully analyzing the wind and temperature fields at each of these levels. Then a differential advection term, similar to that of Fujita and Bradbury (1966) was computed:

$$D. A. = (-\vec{V} \cdot \nabla_H T)_{500} - (-\vec{V} \cdot \nabla_H T)_{700} \quad (7)$$

where negative values of differential advection (D. A.) represent steepening of the lapse rate.

On 5 August, 1967, most of the activity that eventually produced hailstorms organized near the tri-state border area between Cheyenne, Wyoming and Sydney, Nebraska. Strong convective activity also occurred in the mountains to the west and in northern Nebraska. Kansas remained relatively clear.

Figure 14 gives a composite of the values of differential advection computed for 5 August, 0500 MST, along with the convective activity that took place nine hours after the computational period (1400 MST). The first reported hail occurred at that time. The surface weather is based on the hourly surface observations made by the U. S. Weather Bureau and FAA stations. It can be seen that, except for the mountain areas, there is some agreement between the magnitude of destabilization of the atmosphere and the degree of convective activity. The differential advection may have occurred due to upper-level cold air advection blowing over southwest winds, warmed by the mountains, which act as an effective elevated heating source.

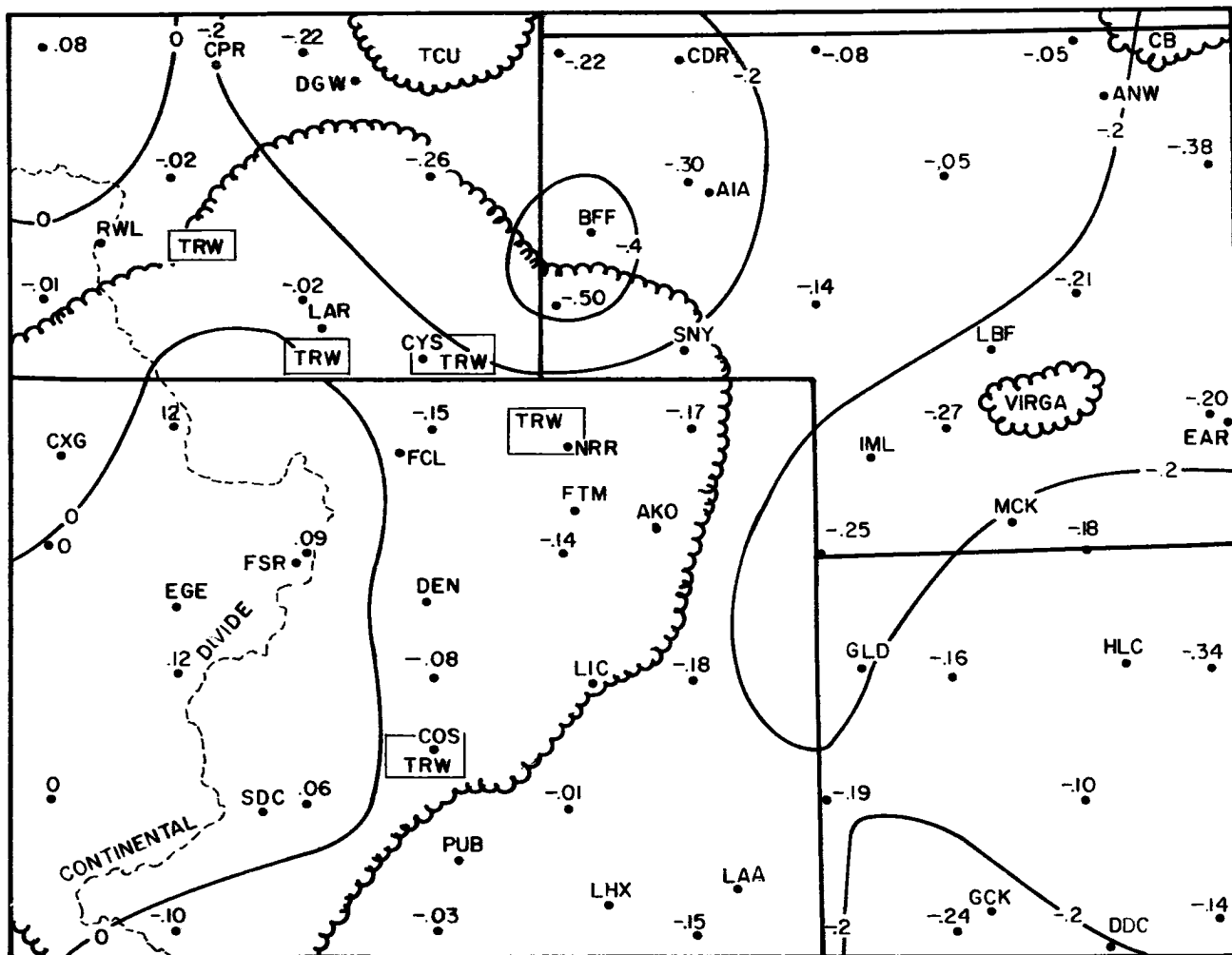


Figure 14: Values of horizontal differential temperature advection in  $^{\circ}\text{C}\text{-hour}^{-1}$  analyzed for 0500 MST, 5 August, 1967, and the surface weather that occurred nine hours later (1400 MST).

If it is assumed that the error in radiosonde measurements is  $\pm 5$  knots in wind velocities and  $\pm 10^\circ$  in wind direction, there is approximately a 38% error in the computed value of advection for  $-\mathbf{V} \cdot \nabla_H T$  in the vicinity of  $0.40^\circ\text{C}\text{-hour}^{-1}$ . This is assuming an accurate isogon and isotach analysis and an accurate temperature gradient analysis. If it is further assumed that a temperature gradient analysis could be in error by  $\pm 1^\circ\text{C}$  (due possibly to instrument errors) over 100 miles, then the error is over 100%; i.e.,  $0.40 \pm 0.65^\circ\text{C}\text{-hour}^{-1}$ . If errors were this high, then obviously the computations would be meaningless. However, it is believed that isogon, isotach, and temperature analyses were done quite accurately for the given data, and that errors are less than used in the above latter example. The largest source of error is the sparseness of data for the type of computation desired.

The relative values among the grid points are probably more accurate than the absolute values. Thus, the fields of positive and negative differential advection values more clearly represent destabilization processes than the absolute value at any given grid point.

To compare the values of differential advection on 5 August with other days, differential temperature advection was computed for the period 25 July to 5 August. The advection values were compared with the actual temperature changes that occurred at those levels at the rawinsonde stations that lie within the grid network. Less than 50% of the computations predicted the 12-hour temperature changes that actually occurred at the rawinsonde stations. This is understandable, however, when the changes that can occur due to convection and large scale vertical motions, as well as computational errors, are considered. The station with the best correlation between computed and actual temperature change was New Raymer. Furthermore, the computations predicted the actual temperature changes more accurately on dry days than on strong convective days.

Other authors have also investigated the destabilization of the atmosphere due to horizontal advection of parameters. Fujita and

Bradbury (1966) use the 850 mb wind as the coordinate and show that areas of strongest destabilization correspond with the areas of tornado development in the Palm Sunday tornado situation of 11 April, 1965.

Miller (1955) hypothesizes that vertical instability produced by horizontal differential advection would act on a precipitation system to increase the total amount of precipitation and to cause high intensities of precipitation over short periods of time. By forecasting a stability index similar to Showalter's (1953) over a grid by advection of parameters, and comparing with actual precipitation amounts, he verifies the second half of his hypothesis.

Appleby (1954) makes a similar study in which he advects forecasts of the 850 mb temperature and dew point and 700 mb temperature to get a stability index at 700 mb. He then compares forecasted values of this stability index, 850 mb dew points, and the Laplacian of the 850 mb temperature advection with actual precipitation, and gets good results. His differential advection is the Laplacian of temperature, and not the vertical change of temperature referred to above.

In a similar study Whitney and Miller (1956) attempt to show that differential advection alone is sufficient to destabilize the sounding such that tornadoes may form. They show that differential advection destabilized the Mt. Clemens, Michigan, sounding of 8 June, 1953 (a tornado day) to the point that nearly zero energy was required to lift a parcel to the level of free convection.

Chapter V  
APPLICATION OF RESULTS TO HAIL FORECASTING

Summary of Results

It has been shown that the low-level moisture supply is of prime importance in the formation of hailstorms. This in turn results in a low convective condensation level. A CCL below the 650 mb level is a good indicator of instability.

Stability indexes are useful numbers to help with making forecasts, but they cannot give concrete answers. A lifted index with values of less than -2 is a strong indicator that hail will occur. If values are greater than zero hail rarely occurs.

If the total energy profile (or, similarly, the  $\theta_e$  profile) could be evaluated from a sounding representative of the area, using forecast afternoon values in the lower layers, a better idea of the type of stability on a given day may be determined. From an examination of 40 rawinsondes launched at New Raymer, Colorado in the summer of 1967 it was found that the average Total Energy Index, as defined above, was 5480 joules for hail days and 3620 joules for no hail days.

It has been shown that synoptic scale disturbances may be important in the formation of hailstorms, and should be carefully evaluated by the forecaster. In particular, some form of surface convergence in connection with a plentiful supply of low-level moisture is a good indication that severe convective activity will occur. This may be reflected aloft as a certain increase in baroclinicity. The surface cyclonic circulation may actually act as the mechanism whereby instability is increased, with the cyclonic circulation advecting in Gulf moisture from the east and south.

Advection processes on a scale smaller than synoptic scale could be of importance in forming convective activity. However, these processes are difficult to determine from available upper air data. Probably the best indicator of advective processes is the low level moisture as determined by surface dew points and surface wind directions over a large area, and upper air temperature changes as determined from

the 500 mb chart. It was shown at the beginning of this paper that dew points at the surface of greater than 49°F in the northeastern Colorado area are usually necessary before summertime hailstorm activity can be considered.

#### Application of Results to Specific 1968 Cases

The results of the preceding chapters may be summarized in a "Forecasting Table" similar to that of Miller (1967b) to determine which parameters exist on a given day that may lead to hailstorm formation. These tables include parameters describing the stability of the atmosphere and large-scale disturbances. It also includes an "easterly surface winds" parameter, which implies upsloping motion and advection of moisture from the east. Each parameter is given a rating of "yes" or "no" depending on whether it will or will not contribute to the formation of hailstorms. These tables are shown with the results of six independent cases from 1968. Rawinsonde information from the 1000 MST daily launchings at Ft. Collins was used for the thermodynamic computations since no rawinsondes were launched at New Raymer in 1968. The 0500 MST surface and 500 mb maps were also utilized for the forecast. Figures 15-20 display these maps, and Figure 21 shows the total energy profiles for each 1000 MST sounding.

TABLE 9  
Forecast Table for 22 June, 1968

<u>Parameter</u>	<u>Value</u>	<u>Rating</u>	<u>Reason for Decision</u>
CCL	600 mb	No	1000 MST Sounding
Lifted Index	-3	Yes	1000 MST Sounding
Energy Index	6500	Yes	1000 MST Sounding
Surface Convergence	----	Yes	Dew Point Front
Easterly Surface Winds	----	No	Sfc. Pressure Pattern
500 mb Baroclinicity	----	No	500 mb Contour Pattern

TABLE 10  
Forecast Table for 1 July, 1968

---

<u>Parameter</u>	<u>Value</u>	<u>Rating</u>	<u>Reason for Decision</u>
CCL	650 mb	Yes	1000 MST Sounding
Lifted Index	0	No	1000 MST Sounding
Energy Index	1500	No	1000 MST Sounding
Surface Convergence	----	No	Sfc. Pressure Pattern
Easterly Surface Winds	----	No	Sfc. Pressure Pattern
500 mb Baroclinicity	----	No	500 mb Ridge to West

---

TABLE 11  
Forecast Table for 3 July, 1968

---

<u>Parameter</u>	<u>Value</u>	<u>Rating</u>	<u>Reason for Decision</u>
CCL	655 mb	Yes	1000 MST Sounding
Lifted Index	-5	Yes	1000 MST Sounding
Energy Index	2222	No	1000 MST Sounding
Surface Convergence	----	No	Sfc. Pressure Pattern
Easterly Surface Winds	----	Yes	Sfc. Pressure Pattern
500 mb Baroclinicity	----	No	500 mb Ridge to West

---

TABLE 12  
Forecast Table for 17 July, 1968

---

<u>Parameter</u>	<u>Value</u>	<u>Rating</u>	<u>Reason for Decision</u>
CCL	650 mb	Yes	1000 MST Sounding
Lifted Index	-6	Yes	1000 MST Sounding
Energy Index	6810	Yes	1000 MST Sounding
Surface Convergence	----	No	Sfc. Pressure Pattern
Easterly Surface Winds	----	Yes	Sfc. Pressure Pattern
500 mb Baroclinicity	----	Yes	500 mb Short Wave

---

TABLE 13  
Forecast Table for 19 July, 1969

---

<u>Parameter</u>	<u>Value</u>	<u>Rating</u>	<u>Reason for Decision</u>
CCL	635 mb	No	1000 MST Sounding
Lifted Index	-5	Yes	1000 MST Sounding
Energy Index	7000	Yes	1000 MST Sounding
Surface Convergence	----	Yes	Dew Point Front
Easterly Surface Winds	----	No	Sfc. Pressure Pattern
500 mb Baroclinicity	----	Yes	Weak 500 mb Short Wave

---



TABLE 14  
Forecast Table for 28 July, 1968

<u>Parameter</u>	<u>Value</u>	<u>Rating</u>	<u>Reason for Decision</u>
CCL	685 mb	Yes	1000 MST Sounding
Lifted Index	-3	Yes	1000 MST Sounding
Energy Index	7700	Yes	1000 MST Sounding
Surface Convergence	----	No	Sfc. Pressure Pattern
Easterly Surface Winds	----	Yes	Sfc. Pressure Pattern
500 mb Baroclinicity	----	No	500 mb Ridge to West

The results of these Forecast Tables are shown in Table 15, which also includes the weather that actually occurred on each given day.

TABLE 15  
Summary of results of the Forecasting Tables for  
the six independent 1968 cases.

<u>Date</u>	<u>Parameters</u>		<u>Actual Weather</u>
22 June	3 Yes	3 No	Thundershowers, no hail
1 July	1 Yes	5 No	Clear
3 July	3 Yes	3 No	Moderate, scattered hail
17 July	5 Yes	1 No	Large, scattered hail, funnel clouds
19 July	4 Yes	2 No	Large, wide-spread hail
28 July	4 Yes	2 No	Large, wide-spread hail

These limited data suggest that a combination of parameters, both thermodynamic and dynamic, are necessary for hail to occur. In particular, at least half the parameters should be rated "yes" for a hailstorm to be forecast.

SATURDAY, JUNE 22, 1968

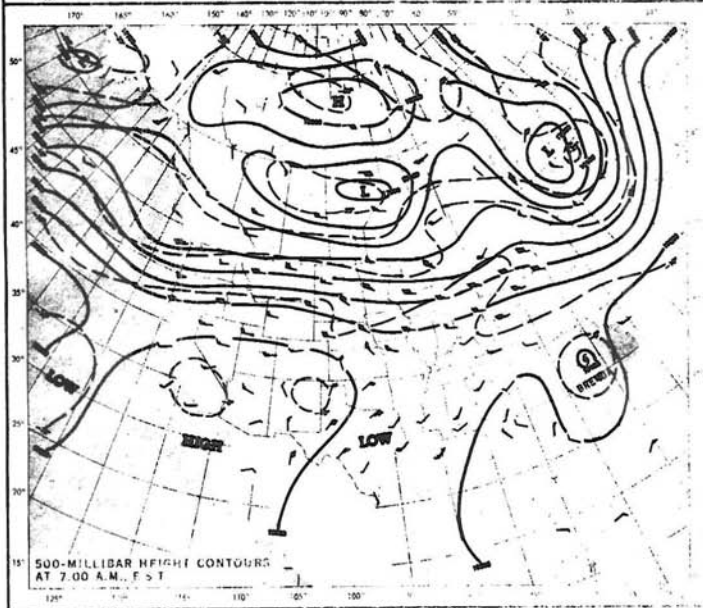
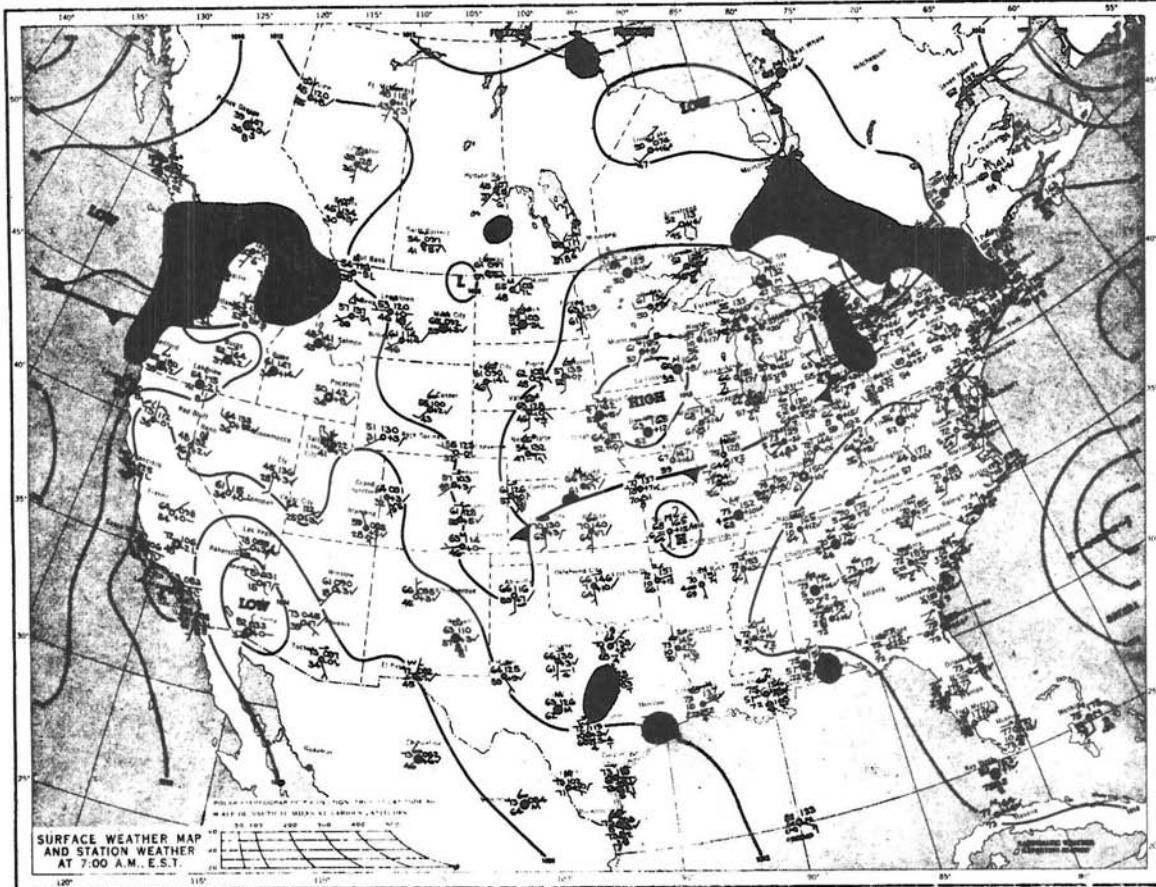


Figure 15: U. S. Department of Commerce ESSA Weather Bureau surface and 500 mb charts for 22 June, 1968, 0500 MST (thundershowers, no hail).

MONDAY, JULY 1, 1968

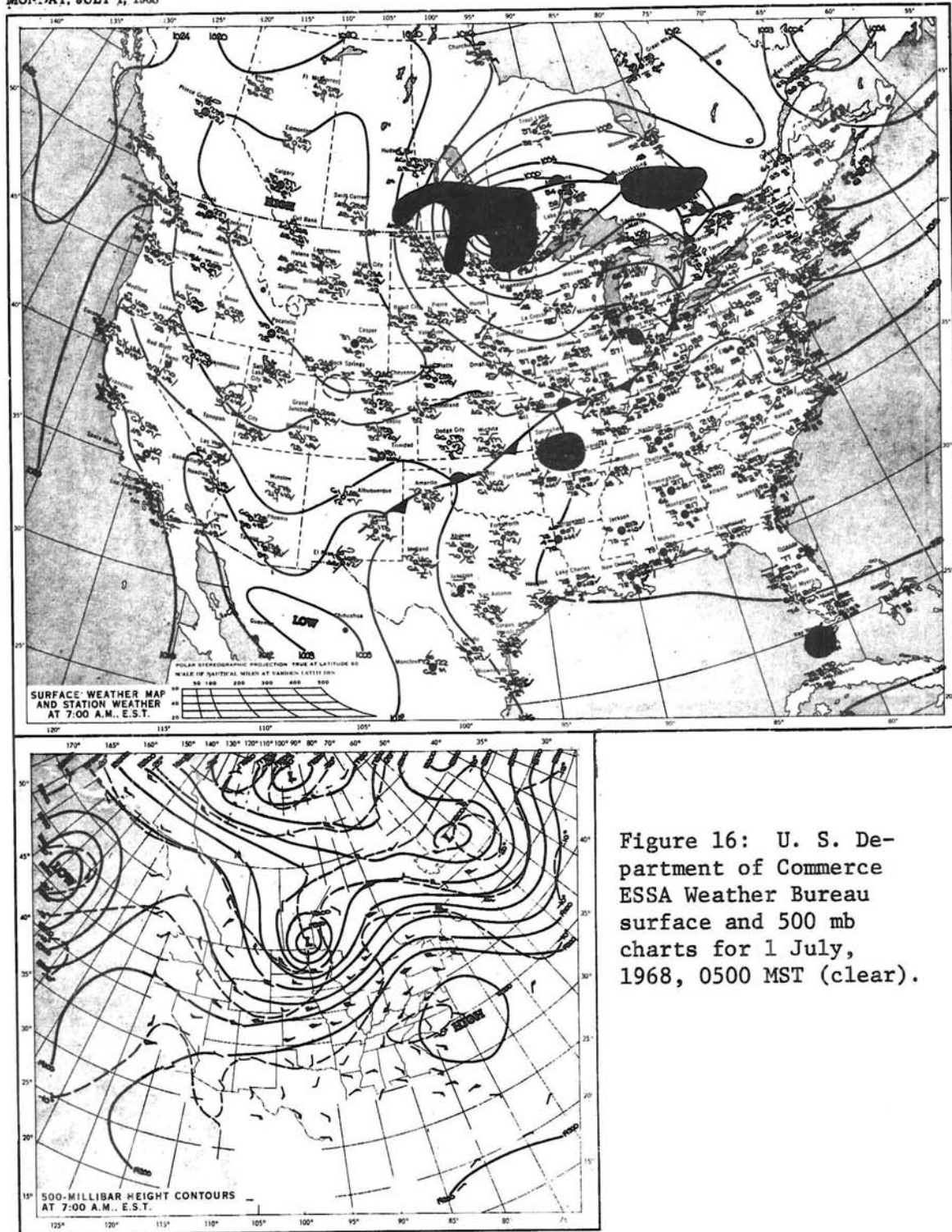


Figure 16: U. S. Department of Commerce ESSA Weather Bureau surface and 500 mb charts for 1 July, 1968, 0500 MST (clear).

WEDNESDAY, JULY 3, 1968

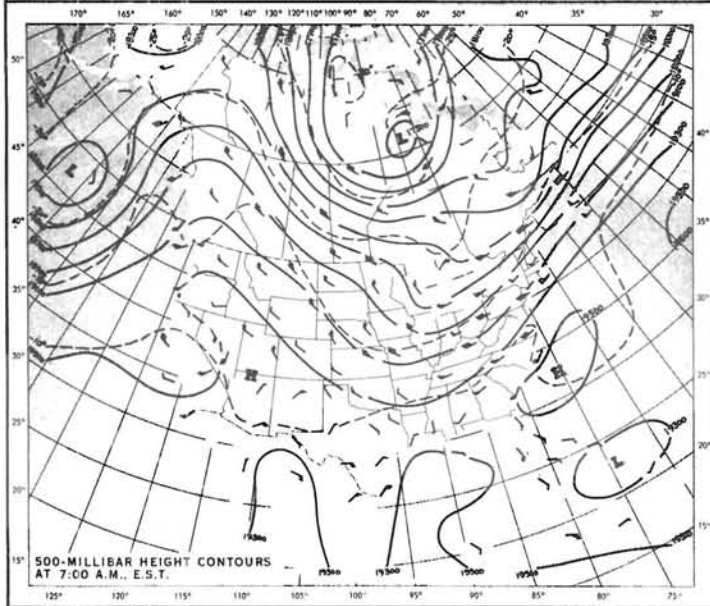
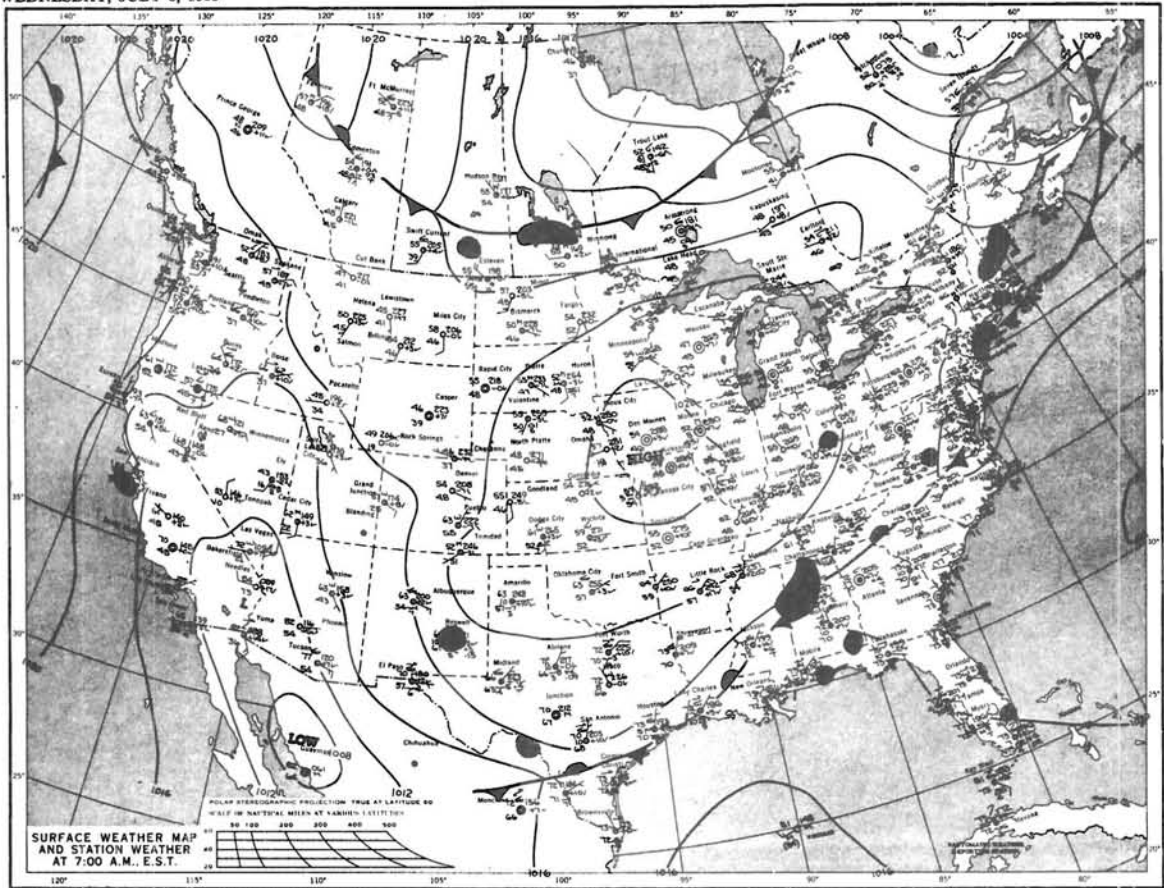


Figure 17: U. S. Department of Commerce ESSA Weather Bureau surface and 500 mb charts for 3 July, 1968, 0500 MST (moderate, scattered hail).

WEDNESDAY, JULY 17, 1968

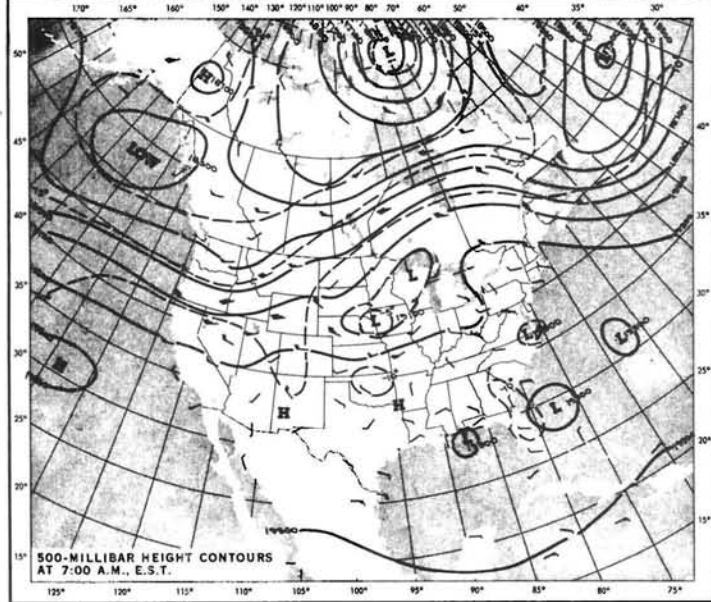
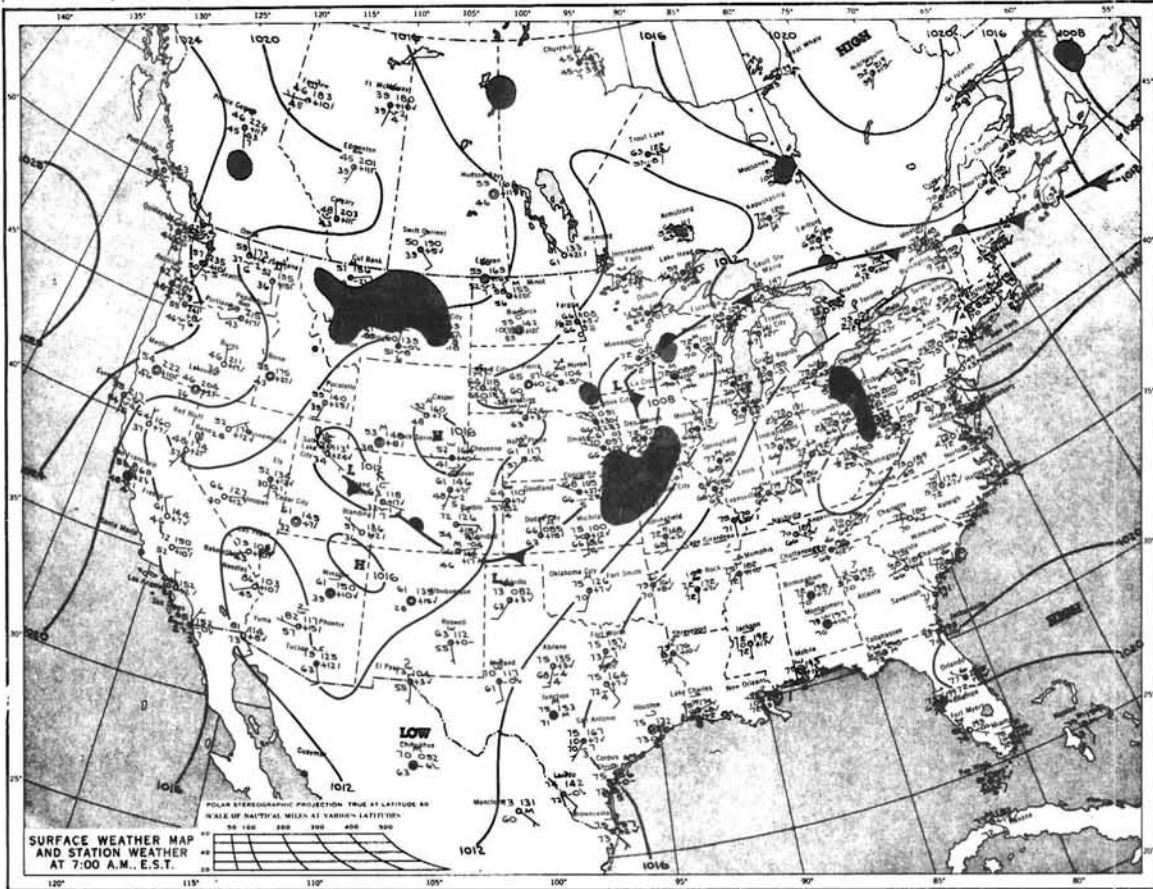


Figure 18: U. S. Department of Commerce ESSA Weather Bureau surface and 500 mb charts for 17 July, 1968, 0500 MST (large, scattered hail, funnel clouds).

FRIDAY, JULY 19, 1968

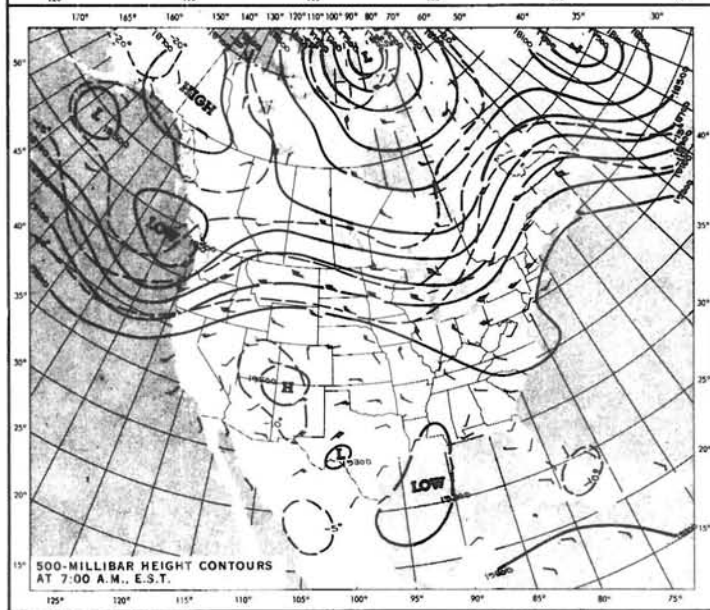
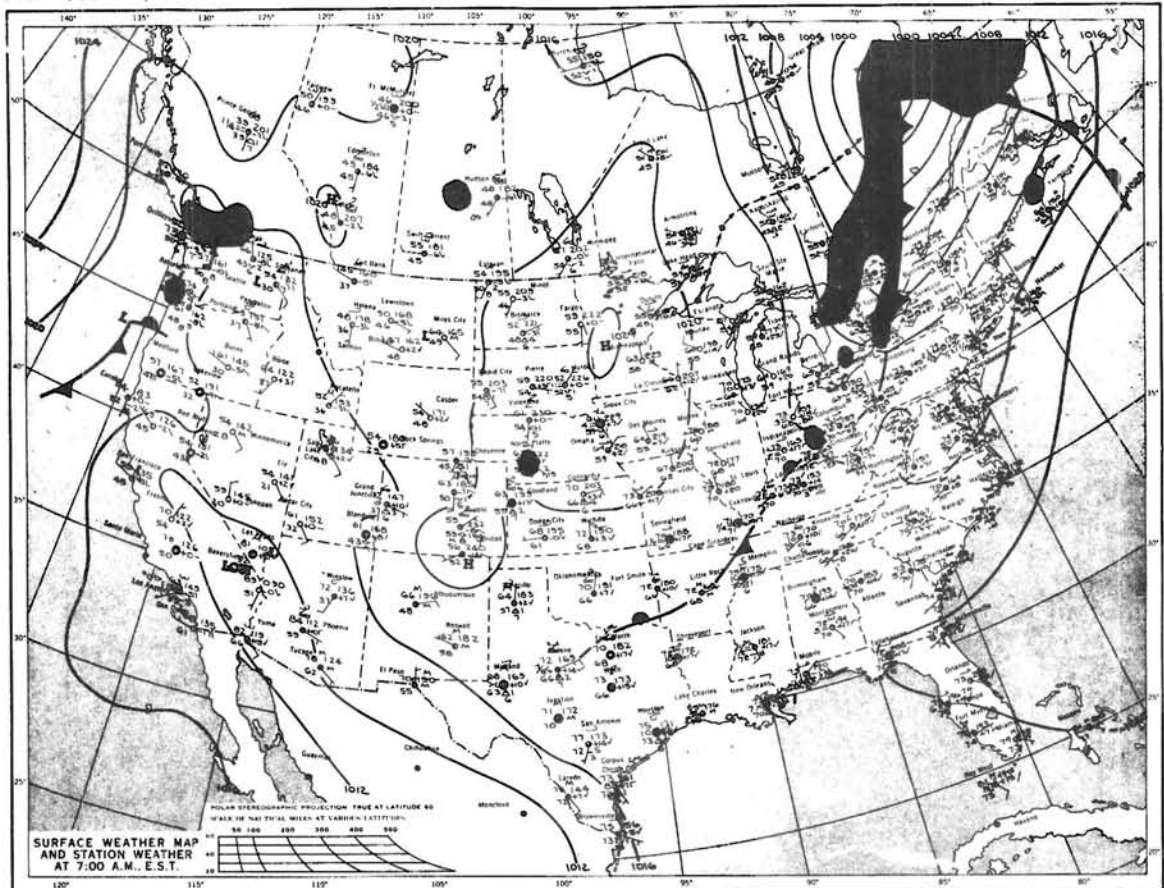


Figure 19: U. S. Department of Commerce ESSA Weather Bureau surface and 500 mb charts for 19 July, 1968, 0500 MST (large, wide-spread hail).

SUNDAY, JULY 28, 1968

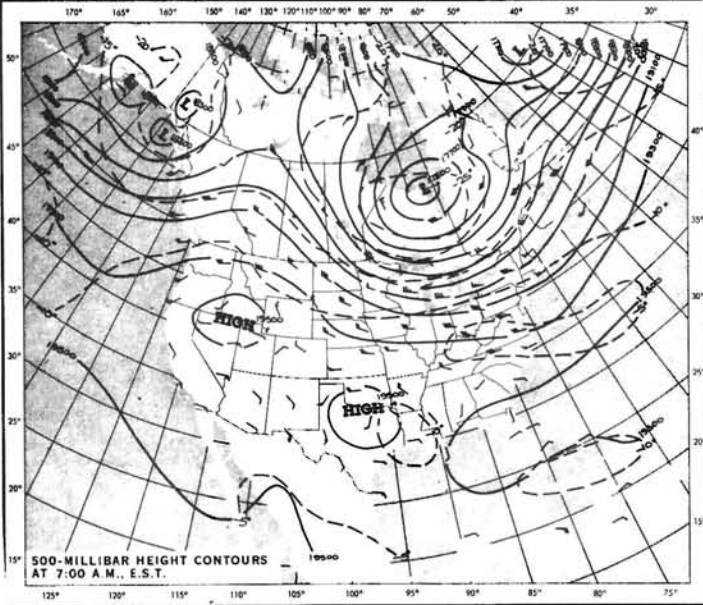
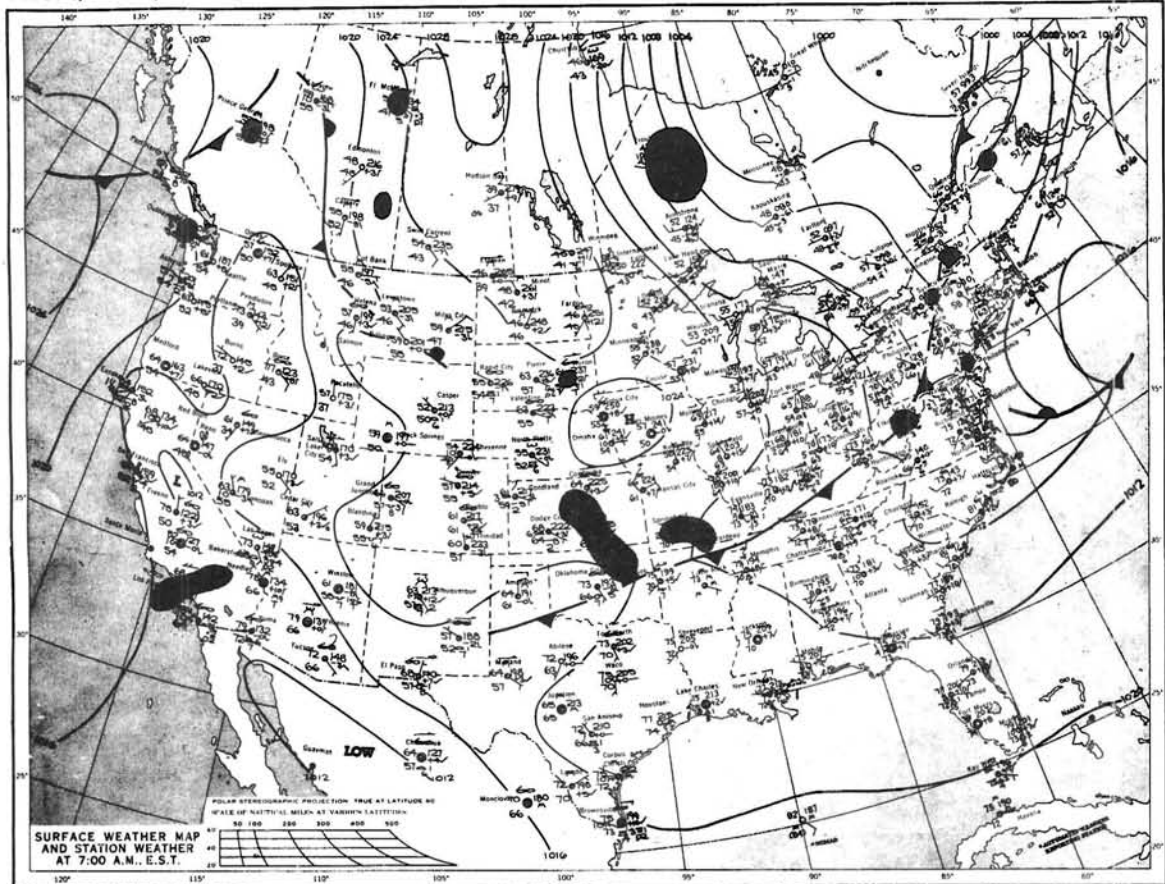


Figure 20: U. S. Department of Commerce ESSA Weather Bureau surface and 500 mb charts for 28 July, 1968, 0500 MST (large, wide-spread hail).

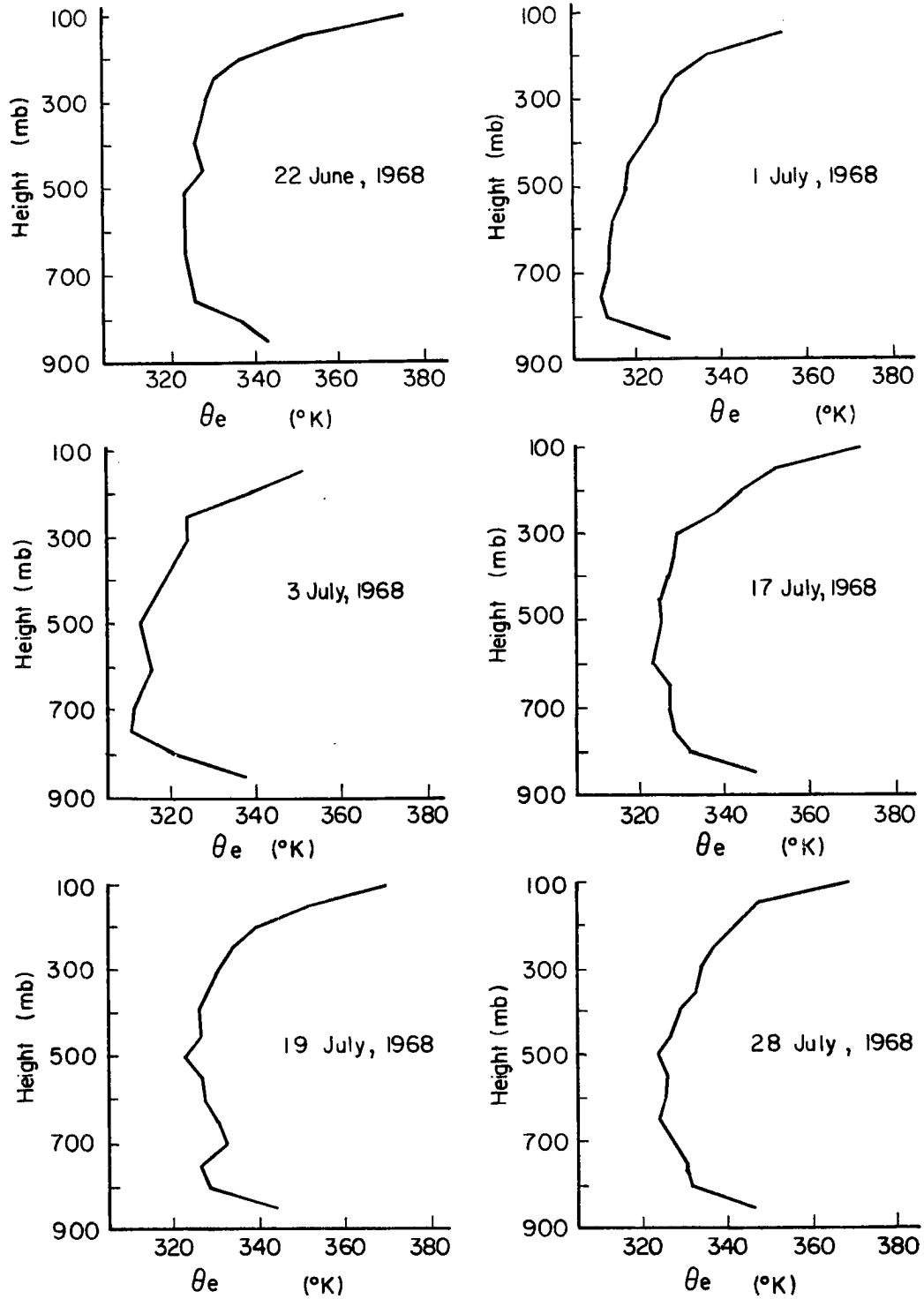


Figure 21: Profiles of equivalent potential temperature  $\theta_e$ ,  $^{\circ}\text{K}$  (or  $E_T$ ,  $\text{joules-gm}^{-1}$ ) for the six independent 1968 cases.



## Chapter VI

### CONCLUSIONS

It has been shown that the low-level moisture is of prime importance in hailstorm formation. From comparison of cloud base measurements with surface parameters, it appears that, assuming parcel theory, the surface mixing ratio is decreased by about 14% at the time a parcel rising dry-adiabatically from the surface reached saturation. The wet bulb freezing level appears to be lower to the ground for large hail days in the high plains than in the midwest. From an examination of total energy profiles, which are essentially the same as profiles of  $\theta_e$ , most of the static energy available for convection is in the very lowest layers of the atmosphere. These profiles also demonstrate that moisture is the prime source for instability, since lapse rates tend to vary little from day to day in the region. However, there is a tendency for lapse rates to be more unstable on hail days.

The presence of surface convergence can act as an important lifting mechanism to initiate convective activity during a conditionally unstable day. The resulting cyclonic circulation at the surface can advect Gulf moisture in from the east and south, thereby increasing the instability. In association with this an increase in baroclinicity aloft may occur due to passage of a trough or short wave. In addition, the stronger winds aloft associated with the baroclinicity can act to increase the intensity of a convective system, as shown by other authors. Thus large-scale disturbances can act to increase the atmospheric instability, provide an initial lifting impetus to convective activity, and produce an environment favorable for intense convective systems.

Horizontal temperature advection may play a role in the formation of hailstorms on a conditionally unstable day by acting to steepen the lapse rates. However, this is very difficult to compute accurately on the mesoscale due to the sparseness of data and analysis errors.

No major advances in the study of hailstorms or in the ability to forecast them can be made without a vast increase in observational and

measuring equipment. A mesoscale wind, temperature and humidity field, with short lapses between the times this information is gathered, would be extremely beneficial in obtaining an accurate analysis of the local environment prior to hailstorm formation. This network can be achieved through a radiosonde system, or through aircraft equipped with temperature and humidity sensing devices and doppler radar. The aircraft can fly specially designed cross-sections to gather this data on a timely basis.

In addition, the low-level relative vorticity and convergence should be studied on a synoptic scale. Along with this the moisture transport over the region should be examined in relation to synoptic disturbances to determine how much the local moisture supply is increased by these large-scale systems.

Since the New Raymer sounding is considered to be typical of the entire region, it would be interesting to determine the vertical gradient of  $\theta_e$  at the exact location of hailstorm formation. This can be done by measurements of long wave radiation at the earth's surface from an airplane to determine surface temperatures over the entire region, and by a mesoscale analysis. It is expected that these local  $\theta_e$  gradients would be much greater than those represented by the New Raymer sounding.

This thesis has attempted to cover only a few aspects of hailstorm formation. As stated above, the vertical wind shear may be very important in the formation of hail. This has been studied recently by Modahl (1969) for northeastern Colorado. Perhaps hailstorm formation requires a delicate balance between the wind shear and the thermodynamic stability on a given day. Certain cloud models that take into consideration particle growth may also be useful in forecasting studies. Further indexes can then be derived that include all important parameters in such a way that forecasting the occurrence of hailstorms can become an almost exacting science.

## LITERATURE CITED

- Appleby, J. F., 1954: Trajectory method of making short-range forecasts of differential advection, instability, and moisture, Monthly Weather Review, 82, 320-334.
- Beckwith, W. B., 1956: Hail observations in the Denver area, U. A. L. Meteorology Circular No. 40, 41 pp.
- Beckwith, W. B., 1960: Analysis of hailstorms in the Denver network, 1949-1958, Geophysical Monographs No. 5, Physics of Precipitation, American Geophysical Union, pp. 348-353.
- Beers, N. R., 1945: Meteorological thermodynamics and atmospheric statics, Section V of Handbook of Meteorology, F. A. Berry, E. Bolla, and N. R. Beers, ed., McGraw Hill Book Co., Inc., New York, 314-409.
- Darkow, G. L., 1968: The total energy environment of severe storms, Journal of Applied Meteorology, 7, 199-205.
- Das, P., 1962: Influence of wind shear on the growth of hail, Journal of the Atmospheric Sciences, 19, 407-414.
- Dessens, H., 1960: Severe hailstorms are associated with very strong winds between 6000 and 12,000 meters, Geophysical Monographs No. 5, Physics of Precipitation, American Geophysical Union pp. 333-338.
- Fawbush, E. J. and R. C. Miller, 1953: A method for forecasting hailstone size at the earth's surface, Bulletin of the American Meteorological Society, 34, 235-249.
- Fujita, T. and D. L. Bradbury, 1966: Stability and differential advection associated with tornado development, S. M. R. P. Research Paper No. 52, Department of Geophysical Sciences, The University of Chicago.
- Galway, J. G., 1956: The lifted index as a predictor of latent instability, Bulletin of the American Meteorological Society, 37, 528-529.
- Haltiner, G. J. and F. L. Martin, 1957: Dynamical and Physical Meteorology, McGraw Hill Book Co., Inc., New York, 470 pp.
- Harrison, H. T. and W. B. Beckwith, 1951: Studies on the distribution and forecasting of hail in western United States, Bulletin of the American Meteorological Society, 32, 119-131.
- Hodges, H., 1959: Synoptic patterns associated with hail occurrence in northeastern Colorado, National Science Foundation Research Participation Report, Colorado State University, Ft. Collins, Colorado, 77 pp. CER59HH29. Unpublished.

- House, D. C., 1958: Air-mass modification and upper-level divergence, Bulletin of the American Meteorological Society, 39, 137-143.
- House, D. C., 1961: The divergence equation as related to severe thunderstorm forecasting, Bulletin of the American Meteorological Society, 42, 803-816.
- House, D. C., 1963: Forecasting tornadoes and severe thunderstorms, Meteorological Monographs No. 5, 141-155.
- Longley, R. W. and C. E. Thompson, 1965: A study of the causes of hail, Journal of Applied Meteorology, 4, 69-82.
- Marwitz, J. D., 1966: The relation of convective intensity to thermodynamic instability in the high plains, Paper prepared during part of a 15-day active duty tour at Detachment 6, 24th Wea Sqdn, Lowry AFB, Colorado, 11 pp.
- Miller, J. E., 1955: Intensification of precipitation by differential advection, Journal of Meteorology, 12, 472-477.
- Miller, R. C., 1967a: Notes on analysis and severe-storm forecasting procedures of the military weather warning center, Technical Report 200, Air Weather Service, United States Air Force.
- Miller, R. C., 1967b: "Semi-objective evaluation of the relative importance of parameters favoring production of severe local storms," Proceedings of the Conference of Severe Local Storms of the AMS, St. Louis, Missouri, October 19-20, 1967.
- Modahl, A. C., 1969: "The influence of vertical wind shear on hail-storm development and structure," Master's Thesis, Colorado State University, Fort Collins, Colorado.
- Newton, C. W. and H. R. Newton, 1959: Dynamical interactions between large convective clouds and environment with vertical shear, Journal of Meteorology, 16, 483-496.
- Normand, W. W. B., 1938: On stability from water vapor, Quarterly Journal of the Royal Meteorological Society, 64, 47-66.
- Normand, W. W. B., 1946: Energy in the atmosphere, Quarterly Journal of the Royal Meteorological Society, 72, 145-167.
- Ratner, B., 1961: Do high-speed winds aloft influence the occurrence of hail? Bulletin of the American Meteorological Society, 42, 443-446.

- Schleusener, R. A., 1962: On the relation of the latitude and strength of the 500 mb west wind along 110° W longitude and the occurrence of hail in the lee of the Rocky Mountains, Colorado State University Atmospheric Science Technical Paper No. 26, Fort Collins, Colorado, 20 pp., CER61RAS46.
- Schleusener, R. A., 1963: Analysis of synoptic data for selected hail days in northeastern Colorado, 1961, Final Report, NSF Grant G-17964, Civil Engineering Section, Colorado State University, Fort Collins, Colorado, CER63RAS34.
- Schleusener, R. A. and A. H. Auer, Jr., 1964: Hailstorms in the high plains, Final Report, NSF Grant G-23706, Civil Engineering Section, Colorado State University, Fort Collins, Colorado, 100 pp., CER64RAS36.
- Showalter, A. K., 1953: A stability index for thunderstorm forecasting, Bulletin of the American Meteorological Society, 35, 250-252.
- U. S. Department of Commerce, ESSA Daily Weather Maps, Weekly Series: 17-23 June, 1-7 July, 15-21 July, 22-28 July, 1968, U. S. Government Printing Office, Washington, D. C.
- Whitney, L. F. and J. E. Miller, 1956: Destabilization by differential advection in the tornado situation of 8 June, 1953, Bulletin of the American Meteorological Society, 37, 224-229.